Species Discrimination and Monitoring of Abiotic Stress Tolerance by Chlorophyll Fluorescence Transients

Anamika Mishra
University of South Bohemia, Institute of Physical Biology

A thesis submitted to the University of South Bohemia
in partial fulfillment of the requirement for the degree of

Doctor of Philosophy

Supervisor: Doc. RNDr. Ladislav Nedbal, Dr.Sc.
CzechGlobe - Global Change Research Centre, v.v.i.
Academy of Sciences of the Czech Republic,

Nové Hrady
2011

Mishra Anamika, 2011: Species Discrimination and Monitoring of Abiotic Stress Tolerance by Chlorophyll Fluorescence Transients. PhD thesis – 107 pages, University of South Bohemia, Institute of Physical Biology, Nové Hrady, Czech Republic

Prohlašuji, že svoji disertační práci jsem vypracovala samostatně pouze s použitím pramenů a literatury uvedených v seznamu citované literatury.

Prohlašuji, že v souladu s § 47b zákona č. 111/1998 Sb. v platném znění souhlasím se zveřejněním své disertační práce, a to v úpravě vzniklé vypuštěním vyznačených částí archivovaných Ústavem fyzikální biologie JČU v Nových Hradech elektronickou cestou ve veřejně přístupné části databáze STAG provozované Jihočeskou univerzitou v Českých Budějovicích na jejích internetových stránkách.

Date: MSc. Anamika Mishra

List of publications

1. A. Mishra, K. Matouš, K. B. Mishra, L. Nedbal. Towards discrimination of plant species by machine vision: Advanced statistical analysis of chlorophyll fluorescence transients. Journal of Fluorescence, 19 (5):905-913, 2009.

2. A. Mishra, K. B. Mishra, I.I. Höermiller, A.G. Heyer, L. Nedbal. Chlorophyll fluorescence emission as a reporter on cold tolerance in *Arabidopsis thaliana* accessions. Plant Signaling & Behaviors, 6(2): 301-310, 2011.

3. K. B. Mishra, R. Iannacone, A. Petrozza, A. Mishra, N. Armentano, G. L. Vecchia, M. Trtílek, F. Cellini, L. Nedbal. Engineered drought tolerance in tomato plants is reflected in chlorophyll fluorescence emission. Plant Science, 2011. doi:10.1016/j.plantsci.2011.03.022

Prohlášení

Nové Hrady, 15.11.2011

Prohlašuji, že M.Sc. Anamika Mishra se podílela na společných publikacích přibližně v níže uvedeném rozsahu.

1. A. Mishra, K. Matouš, K.B. Mishra, L. Nedbal. Towards discrimination of plant species by machine vision: Advanced statistical analysis of chlorophyll fluorescence transients. Journal of Fluorescence, 19 (5):905-913, 2009**. 60%**

2. A. Mishra, K. B. Mishra, I. I. Höermiller, A. G. Heyer, L. Nedbal. Chlorophyll fluorescence emission as a reporter on cold tolerance in *Arabidopsis thaliana* accessions. Plant Signaling & Behaviors, 6(2): 301-310, 2011. **50%**

3. K. B. Mishra, R. Iannacone, A. Petrozza**,** A. Mishra, N. Armentano, G. L. Vecchia, M. Trtílek, F. Cellini, L. Nedbal. Engineered drought tolerance in tomato plants is reflected in chlorophyll fluorescence emission. Plant Science, 2011. doi:10.1016/j.plantsci.2011.03.022. **15%**

Doc. RNDr. Ladislav Nedbal, Dr.Sc.

Acknowledgements

I am grateful to my advisor Ladislav Nedbal for his inspiring suggestions, discussions and efficient guidance throughout my study. His broad view on the subject along with fruitful and extensive comments made it possible for me to complete the related research articles, and this had a direct impact on the quality of my PhD thesis. My special thanks belong to Karel Matouš for enhancing my knowledge of statistical techniques and MATLAB programming. I sincerely express my gratitude to my colleagues Julie Olejníčkova, Kumud B. Mishra, Josef Lazàr, Zuzana Benedikty, Radek Tesař, Alexey Bonder and David Šebela for their scientific as well as personal assistance during my stay at Nové Hrady.

I acknowledge Arnd G. Heyer (University of Stuttgart, Germany) for his interest in our work and for offering me a short term visit to his laboratory to complete part of my experimental work. I also thank Rina Iannacone (Agrobios, Metaponto (MT), Italy) for her collaboration in another project.

I am thankful to Govindjee (University of Illinois, USA) for his comments and suggestions during his visits to Nové Hrady. I express my sincere thanks to Pranav Mishra (IBM, USA) for critical reading of this thesis.

I would like to acknowledge my friends Vasilina Zayats, Tatyana Prudnikova and Oksana Degtjarik and many others for their interactions. At last but not the least, I thank all the staff of UFB, USBE and CzechGlobe for taking good care of me and my family whenever we needed anything during my study period.

My parent's constant encouragement at early stage of my life started me down the road to a career in studies and research. I am gratefully obliged to my parents, in-laws, brothers and sisters for their constant support. Without it, it would have been impossible to complete this work while staying away far from them. I adore my husband Kumud B. Mishra for his cooperation in accomplishing this work.

This thesis is dedicated to

my Mom and Dad

Table of Contents

List of Figures

Figure 6. *The Jablonski diagram showing chlorophyll fluorescence of plants competes with photosynthesis for excitation energy. When Chl a molecule absorbs light, it is excited to higher energy levels (S_2), before rapidly relaxing to the lowest excited energy level (S_1). This relaxation event is called vibration relaxation and occurs in much less than picoseconds. The transition from the higher excited state to the ground state (S_0) that leads to light emission is termed fluorescence. In the singlet excited state (S_1), the spins of the electrons are antiparallel; however, if there is a spin conversion, and we have parallel spins, the molecule goes into a triplet state (T_1). Phosphorescence occurs when the electron returns to the ground state from this triplet state by intersystem crossing; this process is much slower than fluorescence. Source: Inspired by http://www.olympusmicro.com/primer/java/jablonski/jabintro/index.html*

Figure 7. *Experimental **p**rotocol for the chlorophyll fluorescence quenching analysis using modulated light. A dark-adapted leaf is exposed to two flashes of saturating light in continuous actinic light and two flashes of saturating light in dark.*

Figure 8. *Euclidean distance between two images $f(t_k)$ and $f(t_m)$ in two dimensional space. Source: Inspired by, http://en.wikipedia.org/wiki/Euclidean_distance*

Figure 9. *Dark region shows the area with the same Mahalanobis distance to the full set of X image sequence. This method takes into account the probability properties of the set X. Source: Inspired by, http://www.aiaccess.net/English/Glossaries/GlosMod/e_gm_mahalanobis.htm*

Figure 10 *Linear Discriminant Classifier (LDC) in a 2-dimensional feature space. The training class C_1 is characterized by a low F_0 (=$f(t_1)$) and a high F_V (=$f(t_2)$), e.g., in pixels capturing emission from photosynthetically active leaf regions. The training class C_2 represents pixels of less photosynthetically active regions. Source: Theodoridis & Koutroumbas 2009*

Figure 11. *Quadratic Discriminant Classifier (QDC) in a 2-dimensional feature space. In QDC, covariance matrixes are different, and the separating line is shown quadratic. Source: Inspired by, http://cmp.felk.cvut.cz/cmp/courses/recognition/Labs/perceptron/index_en.html*

Figure 12.. *The Support Vector Classifier (SVC) in a 2-dimensional feature space. The decision boundary separates the two classes by maximizing the margin. The separating line shown with dark lines and the margin is indicated by dotted lines. Our goal is to search the separating line that gives the maximum possible margin. Source: Inspired by, http://www.emeraldinsight.com/journals.htm?articleid=870666&show=html*

Figure 13. *The Nearest Neighbor Classifier (NNC) in a 2-dimensional feature space. The pixel is found to be closest to the class C_2 and classified as a member of class C_2 after comparing its distance (Euclidian Distance, ED) to the training set (reference) for both classes. Source: Inspired by,*

List of Abbreviations and Symbols

CCD - charge coupled device;

Chl a- chlorophyll a;

Chl b- chlorophyll b;

ChlF - chlorophyll fluorescence;

F_0 - fluorescence emission of a dark adapted plant with primary quinone acceptor Q_A oxidized and non photochemical quenching inactive;

Fisherc - fisher's discriminant classifier;

F_M - fluorescence emission of a dark adapted plant exposed to a brief pulse of a strong light leading to a transient reduction of Q_A without induction of non-photochemical quenching;

F_P - fluorescence peak at the beginning of the transient with actinic light;

F_V - variable fluorescence measured in dark-adapted plants;

F_V/F_M - maximum quantum yield of PSII photochemistry;

IFS - individual feature selection;

k-NNC - k-nearest neighbor classifier;

LT_{50EL}- lethal temperature at which 50% of electrolyte leakage occurs;

LDC- linear discriminant classifier;

Neurc - artificial neural networks classifier;

NMC - nearest mean classifier;

NNC- nearest neighbor classifier;

NPQ - non-photochemical quenching of excited state of a molecule;

PQ- Plastoquinone;

PS I - Photosystem I;

PS II- *Photosystem II;*

Q_A, - *primary quinone accepter of PSII;*

Q_B - *secondary quinone acceptor of PSII;*

QDC - *quadratic discriminant classifier;*

qP - *photochemical quenching;*

Rfd **-** *fluorescence decrease ratio (plant vitality index)*;

SVC - *support vector classifier;*

SFFS - *sequential forward floating selection;*

SFS - *sequential forward selection;*

SBS - *sequential backward selection;*

Φ_{PSII} - *effective quantum yield of PSII photochemistry.*

Annotation

Chlorophyll fluorescence imaging has become a versatile and standard tool in fundamental and applied plant research. This method captures two dimensional time series images of the chlorophyll fluorescence emission at the leaf surface or whole plants upon various illuminations, typically combination of actinic light and saturating flashes. Several standard chlorophyll fluorescence parameters have been recognized that have physiological interpretation and are useful for, e.g., assessment of plant health status and early detection of biotic and abiotic stresses. The standard fluorescence utilizes well defined single image such as F_0, F_p, F_m, F_s or arithmetic combinations of basic images such as F_v/F_m, Φ_{PSII}, NPQ, qP. Images of certain physiologically relevant chlorophyll fluorescence parameters allowed us to examine the photosynthetic efficiency of plants, their physiological response in different parts of leaves and in whole plants. Although these standard fluorescence parameters have physiological interpretation, their distribution in the leaf area does not provide information at the early stage of plant stress. However, it is sometimes important to find the most contrasting images of leaves or plants to quantify the stress response at a very early stage. Therefore, we have developed advanced statistical techniques based on statistical classifiers and feature selection methods to select sets of high-contrasting images out of hundreds of captured time series chlorophyll fluorescence images. Combinatorial imaging then used to combine high performing images to create the most contrasting image that represents such an early stage of stress, regardless of their physiological interpretation. Therefore, the application of advanced statistical methods on fluorescence data can succeed in tasks where conventional approaches do not work.

This thesis provides options of using standard chlorophyll fluorescence parameters and advanced statistical methods based on combinatorial imaging (use of classifiers and feature selection methods) for high-throughput screening. We demonstrate the applicability of these approaches in discriminating three species of the same family *Lamiaceae* at a very early stage of their growth. Furthermore, we show that chlorophyll fluorescence imaging can be used for measuring cold and drought tolerance of *Arabidopsis thaliana* and tomato plants, respectively, in a simulated high – throughput screening.

Anotace

Zobrazování kinetiky fluorescence chlorofylu se stalo univerzálním a běžným nástrojem v základním i aplikovaném výzkumu rostlin. Tato metoda zachycuje časovou řadu dvourozměrných obrazů fluorescence chlorofylu v ploše listů nebo celých rostlin v různé ozářenosti; typickým protokolem je kombinace aktinického světla a saturačních pulzů. V minulosti bylo identifikováno několik parametrů fluorescence chlorofylu, které mají fyziologickou interpretaci a jsou důležité např. pro hodnocení zdravotního stavu rostlin a pro včasnou detekci biotického i abiotického stresu rostlin. Standardní fluorescenční indexy používají buď jeden základní fluorescenční parametr (F_0, F_p, F_m, F_s), nebo aritmetickou kombinaci základních parametrů (F_v/F_m, Φ_{PSII}, NPQ, qP). Ačkoliv tyto standardní fluorescenční parametry mají fyziologickou interpretaci, jejich distribuce v ploše listu/rostiny nemusí poskytovat informaci o časné fázi stresu rostlin. Proto je někdy důležité najít nejvíce kontrastní obrázky jiných fluorescenčních parametrů tak, aby kvantifikovaly stresovou reakci rostliny v její rané fázi. Pro výběr vysoce kontrastních obrazů fluorescence chlorofylu ze stovek pořízených snímků během časové řady jsme vyvinuli pokročilou statistickou techniku, založenou na klasifikátorech a *feature selection* metodách. Metoda *combinatorial imaging* vyvinutá v naší laboratoři využívá kombinaci několika obrázků fluorescenčních parametrů, nezávisle na jejich fyziologické interpretaci, k vytvoření co nejkontrastnějšího obrázku pro potřeby zobrazení např. včasné fáze stresu, rozlišení příbuzných druhů rostlin v porostu apod. Proto aplikace pokročilých statistických metod na fluorescenční data umožňuje uspět v úkolech, kde konvenční přístupy nefungují.

Tato práce se snaží poskytnout srovnání možností využití standardních fluorescenčních parametrů a pokročilých statistických metod (použití různých klasifikátorů a *feature selection* metod) aplikovaných na fluorescenční data při snímání vysokého počtu rostlin (High-throughput screening). Demonstrujeme použitelnost těchto přístupů při rozlišení tří druhů stejného rodu *Lamiaceae* ve velmi rané fázi růstu. Dále ukazujeme, že zobrazování fluorescence chlorofylu lze použít při měření tolerance rostlin na chlad a sucho u huseníčku *(Arabidopsis thaliana)* a rajčat, a to v simulovaných high-throughput screeningových pokusech.

Chapter's overview

The first chapter of the thesis reviews the basics of plant photosynthesis and chlorophyll fluorescence. The structural components of photosynthetic apparatus, photosynthetic pigments, and photosynthetic reactions are concisely summarized. We further briefly describe fluorescence in higher plants with a detailed description of chlorophyll fluorescence transients and their parameters.

The second chapter reviews the basics of statistical techniques used for analysis of chlorophyll fluorescence images. Technical details allowing dimensionality reduction of the chlorophyll fluorescence time series are discussed. We further describe the details of the employed classifiers and feature selection methods.

The third chapter describes the plants, materials, and instrumentation comprising imaging FluorCam and experimental protocols.

The fourth chapter presents the main results of this study. The chapter is divided into three sections: 4.1, 4.2 and 4.3.

The section 4.1 demonstrates the discriminative potential of chlorophyll fluorescence imaging in a case study using three closely related plant species of the family *Lamiaceae*. None of the standard fluorescence parameters were able to discriminate between the three species at the early stage of their growth. The potential of eight different classifiers and four feature selection methods was compared in identification of fluorescence features that can yield the highest contrast between the species. This result can be potentially utilized for developing fluorescence based automatic machines that could discriminate crops and weeds at early stages of their growth. This could ultimately lead to a targeted use of agrochemicals.

The section 4.2 demonstrates that chlorophyll fluorescence emission can be instrumental in measuring cold tolerance in *Arabidopsis thaliana* accessions. We used a collection of nine *Arabidopsis thaliana* accessions and compared their fluorescence features with cold tolerance quantified by the well established electrolyte leakage method on detached leaves. We demonstrate that chlorophyll fluorescence parameters: minimal chlorophyll fluorescence, maximum quantum yield of PSII photochemistry and steady state fluorescence normalized to minimal fluorescence are well correlated to the cold tolerance measured by electrolyte leakage methods. In order to further increase the capacity of the fluorescence detection to reveal the low temperature tolerance, we applied combinatorial

imaging. We found that this method, by including the resolving power of several fluorescence features, can be well employed to detect cold tolerance already at mild sub-zero temperatures. The correlation between LT_{50EL} and chlorophyll fluorescence parameters is very convincing for the application of fluorescence based methods in the selection of cold tolerant genotypes.

The last section (4.3) deals with the application of chlorophyll fluorescence in comparing wild type and drought tolerant transgenic tomato line DTL-20, carrying *ATHB*-7 gene. We found that transgenic plants had reduced stomatal density and stomatal pore size, and exhibited an enhanced resistance to soil water deficit. Wild type and transgenic tomato plants were exposed to drought stress lasting for 18 days. The stress was then terminated by rehydration after which the recovery was studied for another 2 days. Plant growth, leaf water potential, and chlorophyll fluorescence were measured during the entire experimental period. The chlorophyll fluorescence parameters: the non-photochemical quenching, effective quantum efficiency of PSII, and the maximum quantum yield of PSII photochemistry yielded a good contrast between the wild type and the transgenic plants from day 7, day 12, and day 14 of water stress, respectively. We suggest that chlorophyll fluorescence emission is an excellent indicator of the level of water stress and, thus, can be used to identify elevated drought tolerance in high-throughput screens for selection of resistant genotypes.

1. Introduction to photosynthesis

1.1 Photosynthesis and components of photosynthetic apparatus

Photosynthesis is a biological process where CO_2 is converted to organic compounds such as sugars by utilizing sunlight. Photosynthesis is a biphasic process taking place in plants, algae and bacteria. In our study we are dealing with C_3 plants. The first phase is called *Light Reactions of Photosynthesis* starts with absorption of light by antenna pigments located in light harvesting complexes (LHCs) of PS II and PS I within the thylakoid membranes of chloroplasts. After absorbing light, primary electron donor chlorophyll *a* (Chl *a*) enters in singlet excited state and transfers its excitation energy to the reaction centers of photosystems (PS II and PS I). There the energy initiates primary photochemical reactions that drive photosynthetic energy conversion. Electron ejected from water splitting gives NADPH and ATP as byproducts. The second phase, *Dark Reactions of Photosynthesis* occurs in the stroma of the chloroplasts. This process uses ATP and NADPH generated by the *Light Reactions* and drives the reduction of CO_2 through Calvin-Benson cycle into sugars (Leegood et al., 2000).

Figure 1 shows a schematic diagram of a typical higher plant showing in descending order of complexity: a leaf, cells, a chloroplast, thylakoid membranes and protein complexes. Chloroplasts organelles in higher plants are normally lens-shaped with dimensions of a few μm (Bradbeer, 1977). The aqueous fluids lying inside the chloroplast are called stroma that includes the enzymes involved in carbon fixation. Stroma contains stacks of thylakoid which host all proteins and pigment-protein complexes necessary for the light-driven reactions of photosynthesis. The stacks of thylakoids are called grana (singular, granum) due to its grain type appearance in the light microscope (Wildman et al., 1980). The grana are connected with each other by stromal lamellae. The compartment bounded by thylakoid membrane is called lumen.

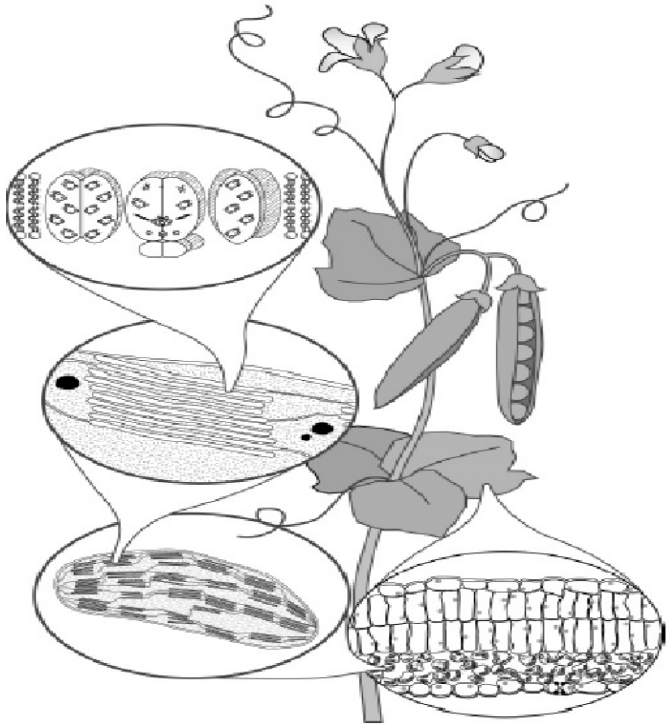

Figure 1. *Schematic presentation of photosynthetic apparatus components in a typical higher plant in descending order of complexity. The first bubble shows a cross-section of a leaf with different types of cells in which the dark spots represent chloroplasts. The second bubble is showing chloroplast in which dark lines are thylakoids and stroma is the stippled area. The third bubble shows grana stack of thylakoids and the fourth bubble includes molecular structure of thylakoid membranes with a reaction center flanked by antenna complexes. Source: Molecular Mechanisms of Photosynthesis, by Robert E. Blankenship, 2002.*

1.2 Photosynthetic pigments

The leaves of higher plants contain several types of photosynthetic pigments: chlorophyll a (Chl *a*), chlorophyll b (Chl *b*) and carotenoids. These photosynthetic pigments capture sunlight that is utilized for photosynthesis. The typical absorption spectra of the photosynthetic pigments (Chl *a*, Chl *b* and carotenoids) are shown in Figure 2. Both chlorophylls show absorption maxima at wavelengths in the blue and red spectral regions.

The Chl *a* possess a methyl group while Chl *b* contains a formyl group at carbon C-7 of the porphyrin ring (Figure 2, right panel). Chl *b* and carotenoids are accessory pigments that only collect sunlight and transport the energy to Chl *a*. Chl *a* not only acts as antenna collecting molecule but also as a primary electron donor in photosynthetic electron transport chain (for details see, section 1.3). Quantitative distribution of Chl *a* and Chl *b* are highly variable with respect to plants species as well as environmental stimuli in higher plants (Kitajima and Hogan, 2003). For example, the ratio of Chl *a*/Chl *b* generally lying from 3.3 to 4.2 in healthy sunlight adapted plants; however, it can be around 2.2 in shade-adapted plants grown at low light (Lichtenthaler, 1987).

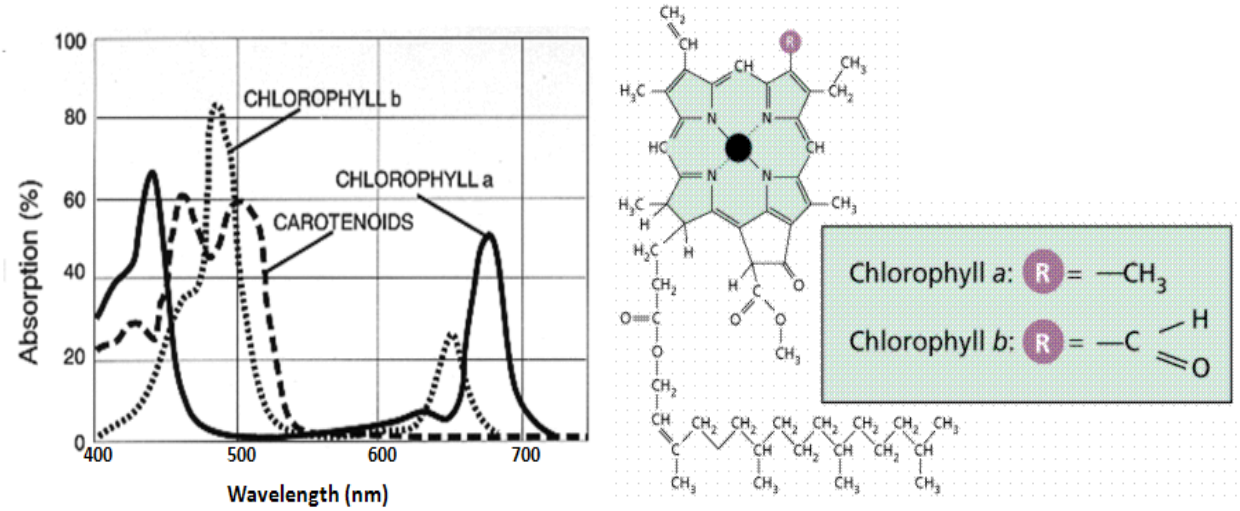

Figure 2. *Left panel illustrates the absorption spectra of photosynthetic pigments: Chl a, Chl b and carotenoids (Source: http://www.life.illinois.edu/govindjee/paper/fig5.gif). Right panel shows molecular structures of Chl a and Chl b. Source: http://classroom.sdmesa.net/eschmid/Lecture19-Microbio.htm.*

Carotinoids are classified into two groups, carotenes and xanthophylls. Carotenes are purely hydrocarbons, while xanthophylls contain hydroxyl groups (oxygenated carotenoids). Thylakoid membranes of higher plants contain small number of carotenoids such as the carotene (ß –carotene), xanthophylls (lutein and neoxanthin) and those participating in the xanthophyll cycle (violaxanthin, antheraxanthin, and zeaxanthin Fig 3, Young, 1993; Demmig-Adams et al., 1996). Inside the thylakoid membranes, carotenoids are linked to

particular chlorophyll carotenoid-binding protein complexes of the Photosystems (Yamamato & Bassi 1996; Demmig-Adams et al., 1996). The distribution of carotenoids within PS I and PS II is highly heterogeneous. Generally, PSI contains higher amount of ß-carotene while PS II is enriched with lutein. The xanthophylls are distributed in rest of the Chl *a*- and *b*-binding, light harvesting antennae (Demmig-Adams et al., 1996). Carotenoids play key role in photoprotection of photosynthetic apparatus under excessive light and contribute to non-photochemical quenching mechanisms (see section 1.5 also; Demmig-Adams et al., 1996; Krause & Jahns 2004). In fact, in nature solar irradiance on the plant surface varies rapidly due to sunflex as well as on a daily and seasonal basis. The xanthophyll cycle, violaxanthin-zeaxanthin interconversions (Fig. 3), is one of the main components taking part in photoprotection by dissipating excessive light and prevents damage of photosynthetic apparatus. In presence of excess light, low thylakoid lumen pH (i.e. high ΔpH) triggers formation of zeaxanthin (Zea) from violaxanthin using enzymes violaxanthin de-epoxidase (VDE, present in thylakoid lumen), and drives protonation of PsbS, a PS II subunit that is necessary for feedback de-excitation (qE) mechanisms (Külheim et al., 2002). Thus, xanthophylls can also participate in de-excitation of singlet excited chlorophyll molecule (^{1}Chl*) and prevent alternative reaction pathways that generates reactive oxygen species (ROS) (Holt et al., 2005). The manipulation of photoprotective pathways can be used to improve the photosynthesis and enhance the productivity of crops in sub-optimal environmental conditions (Murchie & Niyogi 2011).

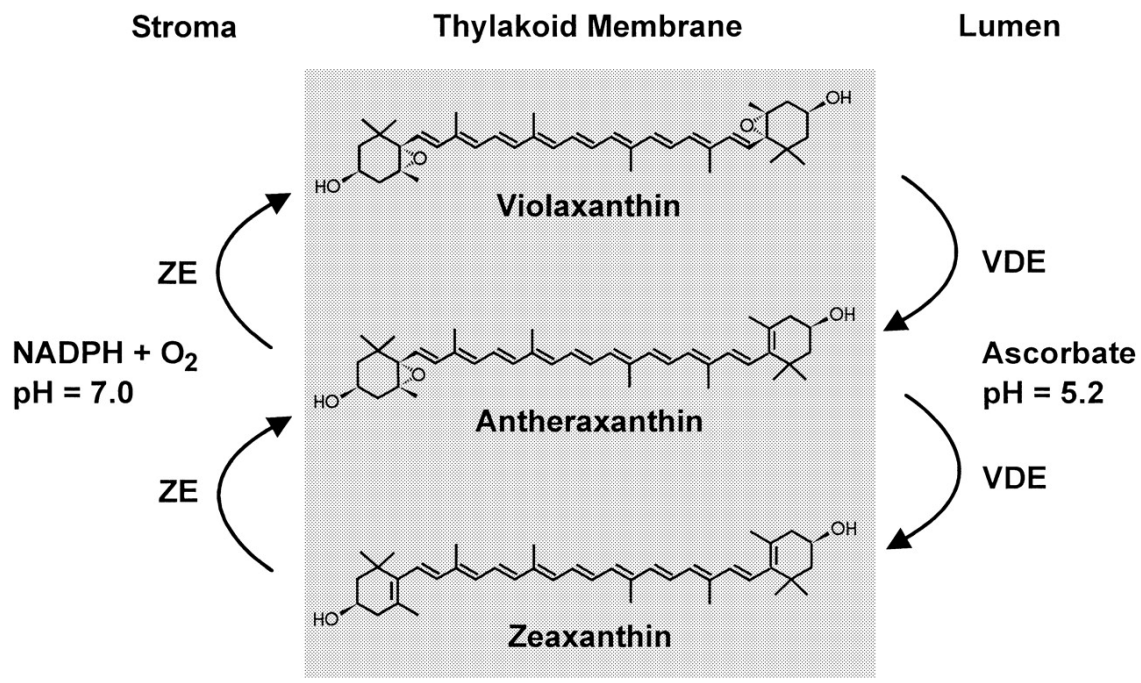

Figure 3. *Xanthophyll cycle representing cyclic conversion of violaxanthin and zeaxanthin. In higher plants, three carotenoid pigments: violaxanthin, antheraxanthin and zeaxanthin are active in the xanthophyll cycle. In presence of high light, violaxanthin is converted to zeaxanthin via the intermediate antheraxanthin. This conversion of violaxanthin to zeaxanthin is catalyzed by the enzyme violaxanthin de-epoxidase (VDE) in lumen while the reverse reaction is performed by zeaxanthin epoxidase (ZE) in stroma of the chloroplast. Source: http://pcp.oxfordjournals.org/content/45/1/92/F1expansion*

1.3 Photosynthetic reactions

Photosynthetic electron transport occurs across and along the thylakoid membranes. Four major protein complexes take part in the light-reactions of photosynthesis (1) Photosystem II (PS II), (2) Cytochrome b_6-f complex (b_6-f complex), (3) Photosystem I (PS I), and (4) the ATP synthase (ATPas**e**), (Govindjee et al., 2010, shown in Fig. 4). These pigment-protein complexes are located in phospholipid-bilayer of the thylakoid membrane. Antenna pigments of the LHCs absorb light and transfer it to Chl *a* molecules that get excited into singlet excited state. The energy of this state is transferred in the form of exitons to reaction center of photosystems where they drive charge separations. The extracted electron from the reaction center of PS II transferred through several electron acceptors (Chl *a*, Pheo *a*, and

Q_A) and finally reached to Q_B. While transferring excitation energy Chl *a* molecule returns to its ground state by getting electron from O_2- evolving complex (OEC) and again waiting to get energy from LHCs. The OEC is bounded with the tyrosine (Yz) residue on the luminal side of PS II. The OEC causes photolysis of water and the removal of O_2 as a byproduct. Recently, the structure of oxygen-evolving PS II is revealed at 1.9 Å resolutions (Umena et al., 2011) and its detailed functioning is reviewed by Kawakami et al. (2011).The electron of Q_B further transferred to the cytochromes b_6f complex through plastoquinone pool. The excitation energy is further transferred to mobile protein plastocynine (PC) which is present in the luminal side to transfer the electrons to PS I. Inside the core of PS I electron that comes from PC is further energized by getting more excitation energy via LHCs of PS I. The electron is transferred from Pollyquinone to Fe-S cluster containing protein located in stromal side. The final step is the catalysis by FNR which reduced $NADP^+$ to NADPH. Other important component of photochemical process of photosynthesis is ATP synthase (ATPase). ATPase synthesizes ATP from ADP and inorganic phosphate using transmembrane ΔpH.

There are two modes of electron transport i.e., linear electron transport and cyclic electron transport. In ***linear electron transportation***, electrons are transferred from water to NADP through Photosystem II (PSII), the cytochrome b_6f complex (cyt bf), and Photosystem I (PSI). However, c***yclic electron transportation*** uses only PSI and cytochrome b_6f (Arnon, 1954). In this process electrons from FNR are transported back to cytochromes b_6f where plastoqunones are again used for the cyclic electron transport. The functioning and the regulatory mechanisms of cyclic electron flow through the transmembrane proteins are still not well understood (Joliet & Johnson, 2011). However, it has been assumed that the linear electron transport generates probably insufficient amount of ATP to balance ATP: NADPH demands in Calvin-Bension cycle and this need is supplemented by cyclic electron transportation (Joliet & Johnson, 2011).

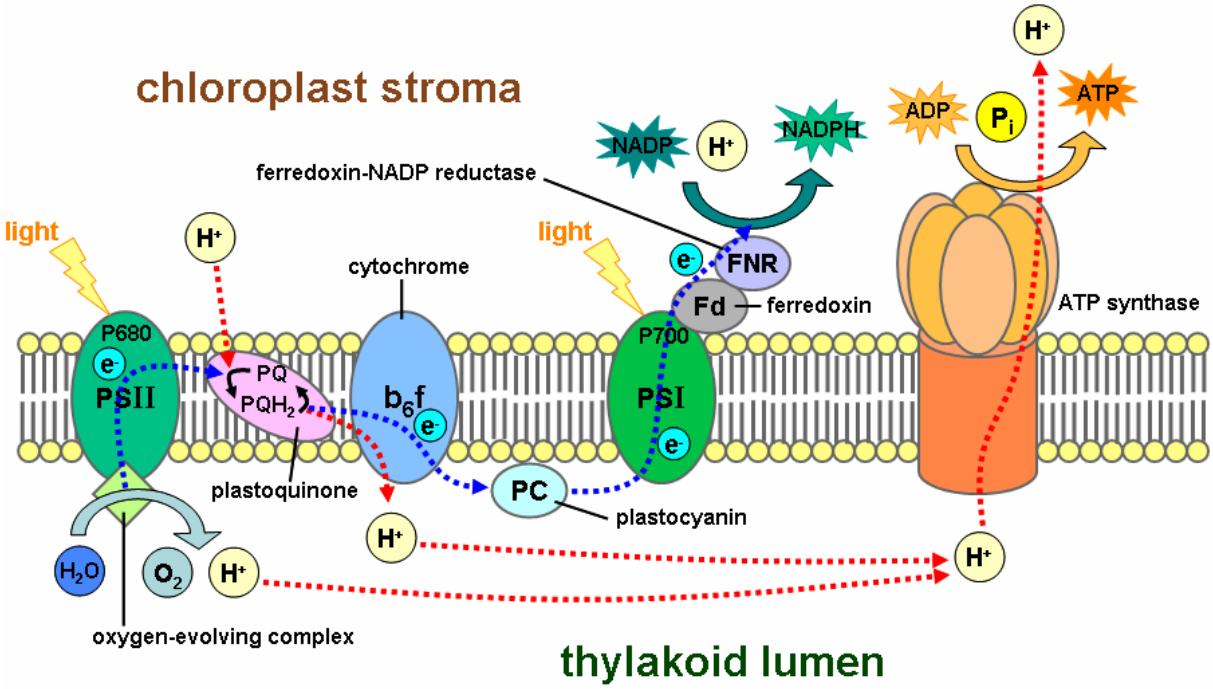

Figure 4. *The scheme of electron transport in oxygenic photosynthesis. The diagram shows linear electron transport in the pigment-protein complexes located in thylakoid membranes of a chloroplast. The energy of absorbed photons is needed to transfer electrons from PS I and PS II donors to their respective acceptors. The electron is further transferred through several electron acceptor/donor pairs, in addition to PS I, PS II, cytochrome b6f (Cyt b_6f), ATP synthase and mobile intersystem electron carriers: plastoquinone (PQ) and plastocyanin (PC). The PQ connects PS II and Cyt b_6f and PC transfers electrons from Cyt b_6f to PS I. Ultimately, the electrons are used for the reduction of $NADP^+$ to NADPH. The holes or the "missing electrons" are supplemented by extracting electrons from water molecules and as a result of the oxidation an oxygen molecule is released as a by-product. By the continuous electron transport, a proton gradient is built across the thylakoid membrane which increases the H^+ (proton) concentration of lumen. Finally, ATP synthase utilizes the proton concentration difference (ΔpH) across the membrane to synthesize ATP by the phosphorylation of ADP. ATP and NADPH are ultimately utilized in the Calvin-Benson cycle, where carbon is assimilated and carbohydrates are synthesized.*
Source: http://en.wikipedia.org/wiki/File:Thylakoid_membrane.png

In *the dark reactions*, the byproducts of light reactions i.e. NADPH and ATP are used for the assimilation of carbon dioxide into carbohydrates via Calvin-Benson cycle. The assimilation of CO_2 occurs in the stroma of the chloroplasts through a complex series of chemical reactions. Ribulose-1,5-Bisphosphate Carboxylase/Oxygenase (RuBisCO) is the key enzyme taking part in catalyzing the first step of CO_2 fixation of the Calvin –Bension cycle. RuBisCO plays important role in both carboxylation and oxygenation reactions. Carboxylation reaction occurs when there is high concentration of CO_2 while oxygenation occurs in presence of high concentration of O_2. During carboxylation reaction endol form of ribulose 1,5-bisphosphate (RuBP) is initially produced that ultimately converted into two molecules of 3- phosphoglycerate (PGA). The oxygenation reactions produced one molecule of each 2-phosphoglycolate and PGA. The product of oxygenation reaction 2-phosphoglycolate inhibits Calvin-Benson cycle and needs to be converted into PGA for further recovery. This process of first oxygenation followed by recovery is collectively known as photorespiration (Heldt, 1997; Oliver, 1998).

C_3 carbon fixation pathway

In ***C_3*** plants, there are three phases to the dark reactions, collectively called the Calvin-Benson cycle, it occurs in the stroma of chloroplasts. These phases are carboxylation (carbon fixation), reduction reactions and RuBP (ribulose 1,5-bisphosphate) regeneration (Blankenship 2002). During carboxylation reaction, the enzyme RuBisCO (Ribulose 1-5 biphosphate carboxylase) catalyses RuBP (Ribulose 1-5 biphosphate, 5 carbon compound) by CO_2 and produce PGA (3-phosphoglycerate, 3 carbon compound). PGA is the first stable intermediate compound of Calvin-Benson cycle. In reduction reactions, enzyme phosphoglycerate kinase catalyses the phosphorylation of PGA by using energy of ATP and NADPH (products of light reaction) and produce 1,3-BPGA (glycerate-1,3-bisphosphate) and ADP as a products. In regeneration reactions, the enzyme G3P (glyceraldehyde 3-phosphate dehydrogenase) catalyses the reduction of 1,3 BPGA by NADPH and produce Glyceraldehyde 3-phosphate. During this process NADPH get oxidized and becomes $NADP^+$

and regenerate RUBP. For the fixation of each CO_2 molecule it requires 2 molecules of NADPH and 3 of ATP and start the cycle again (*http://en.wikipedia.org/wiki/Calvin_cycle*)

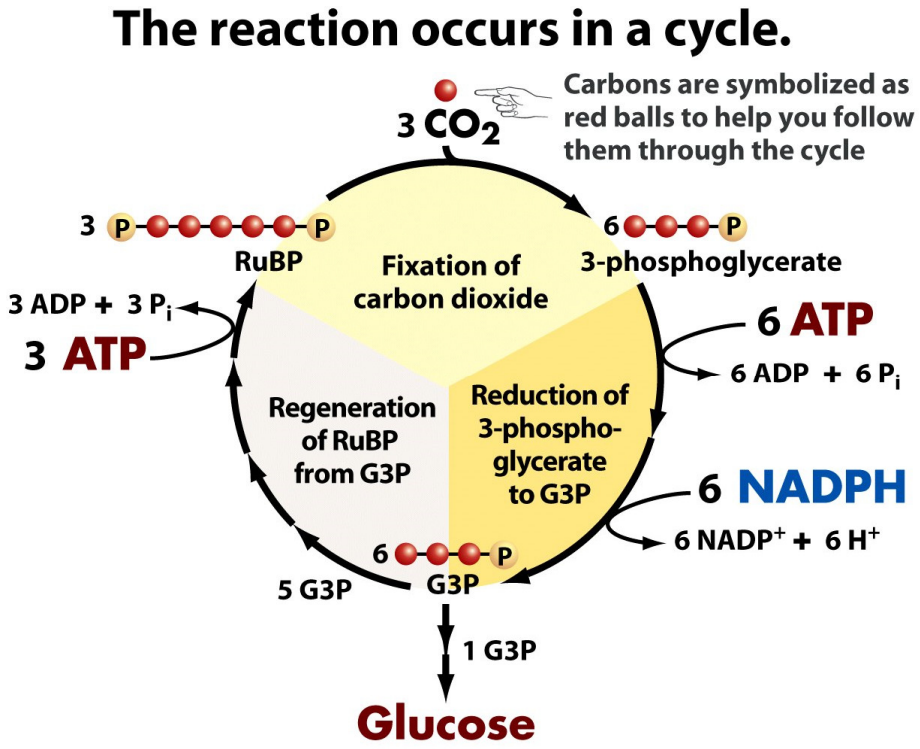

Figure 5. *Carbon fixation through the Calvin-Benson cycle.*
Source: http://www.uic.edu/classes/bios/bios100/f06pm/lect08.htm

1.4 Fluorescence in higher plants

In higher plants, two groups of fluorophores prevail the fluorescence emission spectra. The first group of fluorophores fluoresces in blue-green spectral region with a maximal peak around 440-450 nm and a shoulder at 530 nm when excited with UV light (Buschmann et al, 2000; Mishra & Gopal, 2008 and references therein). This group of fluorophores absorbs most of the UV light in the leaf epidermis and they protect the plants cellular components

(Grossweiner & Smith, 1989), photosystem II (PS II) reaction centers (Rundel 1983) as well as DNA (Stapleton & Walbot, 1994) from the UV damage. The Chl *a* is the second main fluorophore contributing largely to plant fluorescence in the red and near infra-red (NIR) spectral region between 650–800 nm, in two broad bands with maxima lying between 684–695 nm and 730–740 nm (Franck et al., 2002). These fluorescence emission bands are also called red and far-red bands. The red fluorescence band is mostly contributed by PS II complexes (Pfündel 1998). At room temperature, the major portion of far-red fluorescence is from PS II; however, a significant contribution from PS I is reported (Pfündel 1998, Agati et al, 2000). The relative contributions of PS II and PS I fluorescence are varying with decreasing leaf temperature (Agati et al., 2000).

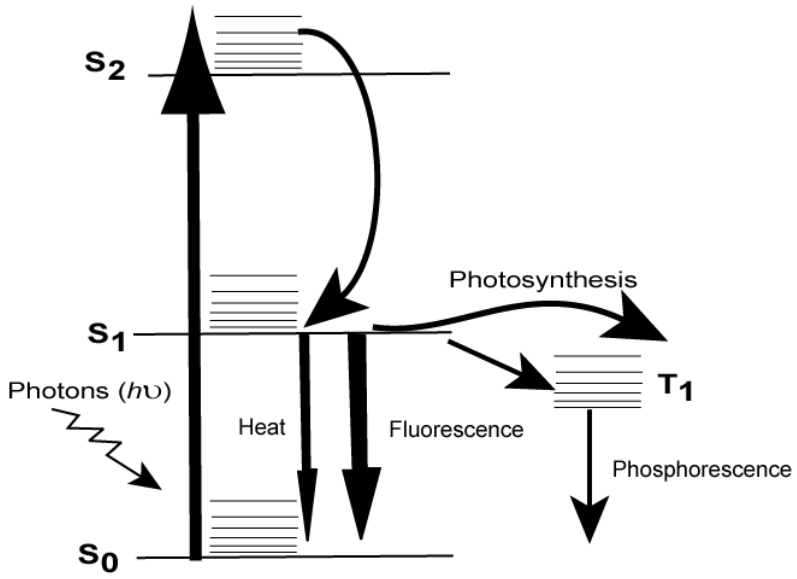

Figure 6. *The Jablonski diagram showing chlorophyll fluorescence of plants competes with photosynthesis for excitation energy. When Chl a molecule absorbs light, it is excited to higher energy levels (S_2), before rapidly relaxing to the lowest excited energy level (S_1). This relaxation event is called vibration relaxation and occurs in much less than picoseconds. The transition from the higher excited state to the ground state (S_0) that leads to light emission is termed fluorescence. In the singlet excited state (S_1), the spins of the electrons are antiparallel; however, if there is a spin conversion, and we have parallel spins, the molecule goes into a triplet state (T_1). Phosphorescence occurs when the electron returns to the ground state from this triplet state by intersystem crossing; this process is much slower than fluorescence. Source: Inspired by, http://www.olympusmicro.com/primer/java/jablonski/jabintro/index.html*

1.5 Chlorophyll fluorescence transient

Contrary to the static blue–green fluorescence, the chlorophyll fluorescence is highly dynamic and provides insight of molecular process of plant photosynthesis occurring at the time scale from femto-seconds to minutes (Nedbal & Koblížek, 2006; Rascher & Nedbal, 2006; Malenovský et al., 2009). The chlorophyll fluorescence transient in between ms to minutes is the most dynamic features of chlorophyll fluorescence so- called Kautsky effect or chlorophyll fluorescence induction kinetics (Kautsky & Hirsch 1931; Govindjee, 1995). Plant chlorophyll fluorescence is emitted primarily from the lowest excited state (S_1) of chlorophyll *a* and competes with photochemistry for excitation energy and heat dissipation (Fig. 6). These three processes e.g, photochemistry, heat dissipation and chlorophyll fluorescence are in competition such that any increase in the efficiency of one will result in a decrease in the yield of the other two. The absorbed lights are predominantly utilized for photochemistry in the reaction centers and only small fraction e.g. 1-2% of it is emitted as chlorophyll fluorescence (Maxwell & Johnson, 2000). However, fluorescence measurement is fairly easy and therefore it is commonly used for the measurements of non-invasive and real time insight into dynamics of photosynthetic reactions. The changes in dynamic of chlorophyll fluorescence emission can probe the functional mechanisms of photosynthetic apparatus and are widely used as a reporter of photosynthetic activity and a regulation in plants (reviewed in several reviews, Kraus and Weis, 1991; Dau 1994; Govindjee, 1995; Lazár, 1999; Nedbal & Koblížek, 2006; Baker, 2008; and in a recent book edited by Papageorgiou & Govindjee, 2004).

The chlorophyll fluorescence transients comprise of two main phases: When the light of high constant intensity is switched on after the plant had been kept in darkness, the fluorescence yield rapidly rises from a minimum value (F_0) to a maximum F_P (or F_M in the case of full Q_A reduction), and it decreases slowly from F_P to a stationary level known as the steady state fluorescence (F_S, Figure 7). Both the rise from F_0 to F_P and the decay after F_P to steady state are characterized by a number of shoulders, inflection points and transient peaks. The shape of the initial rise from F_0 to F_P is polyphasic and it exhibited three (F_J, F_I, F_P;) or four (F_K, F_J, F_I, F_P) phases, respectively, in high light and in heat stress (Strasser et al., 1995; Strasser et al., 1998). The parameters of initial fluorescence rise are highly sensitive to the physiological

state of the plants and may serves as an efficient screening tool (Strasser et al., 2004, Lazàr et al., 2006, Papageorgiou et al., 2007; Stirbet & Govindjee, 2011).

The decrease of the fluorescence yield from the peak F_P to the steady state level F_S is affected by multiple factors including the so called photochemical and non-photochemical quenching. Photochemical quenching (qP) is the decrease of fluorescence yield due to photochemical charge separation (Y_Z P680* Pheo $Q_A \rightarrow Y_Z$ P680$^+$ Pheo$^-$ $Q_A \rightarrow Y_Z^+$ P680 Pheo Q_A^-) in the reaction center (RC II) of photosystem II (PS II). Here, P680* represents the excited singlet state of primary electron donor of PSII; Y_Z is tyrosin Z, the secondary electron donor of PS II; Pheo (*pheophytin a*), the primary electron acceptor from P680*; and Q_A (plastoquinone) the secondary electron acceptor. The most important photochemical quencher is oxidized form of Q_A (Duysens & Sweers 1963). Non-photochemical quenching qN is commonly defined as a quenching of fluorescence not due to photochemical quenching mechanisms (see section 1.2). It is contributed by, among other things, pH gradient at the thylakoid membranes, by state transition qT, and by photoinhibition qI (reviewed in Baker 2008). It is generally assumed that decrease of fluorescence, due to non-photochemical quenching, is caused by an increased loss of energy by thermal dissipation.

Chlorophyll florescence measuring system:

Measurement of the chlorophyll fluorescence of the photosynthetic organism is widely used as a non-destructive tool in photosynthesis research. Introduction of pulse amplitude modulating (PAM) based measuring system (Schreiber et al., 1986) made it possible to measure the fluorescence response in presence of continuous light. Since then various non-imaging and imaging fluorometers have been developed and successfully used for measuring chlorophyll fluorescence transients (Schreiber, 2004). For the measurement of fast phase chlorophyll fluorescence dynamics between F_0 to F_P, plants efficiency analyzer (PEA) is used (Strasser et al., 2004). The first imaging system that enabled to capture images of chlorophyll fluorescence transients was introduced by Omasa et al., (1987). Nedbal et al., (2000a) customized the imaging fluorescence system for field application. Images of physiologically significant fluorescence parameters can provide the source of the heterogeneity in photosynthetic systems that may not be detectable by non-imaging systems. Chlorophyll

florescence imaging systems has provided a powerful means to reveal spatial heterogeneity of leaf photosynthetic performance (Maxwell & Johnson 2000; Nedbal & Whitmarsh 2004; Oxborough, 2004). In addition, fluorescence lifetime imaging microscopy (FLIM) has provided detailed information on the contributions of xanthophyll cycles to Chl *a* fluorescence changes (see e.g., Matsubara et al., 2011, and references therein).

1.6 *Chlorophyll fluorescence parameters*

Pulse Amplitude Modulation (PAM) based chlorophyll fluorescence measuring systems utilize complex light/dark protocols of short measuring flashes, actinic light and high intensity saturating flashes to capture dynamics of chlorophyll fluorescence. Figure 7 shows a typical chlorophyll fluorescence emission response of standard quenching experimental protocol (Schreiber et al., 1986). The controlled excitations using modulated light and precise recording of fluorescence response result in several chlorophyll fluorescence parameters that have physiological significance. In general these fluorescence parameters are divided into two groups: basic parameters and derived parameters. Basic fluorescence parameters can be directly measured while derived fluorescence parameters are constructed from basic parameters. Several reviews have already been published describing detailed physiological significance of basic as well as derived fluorescence parameters (Roháček 2002, Baker 2008).

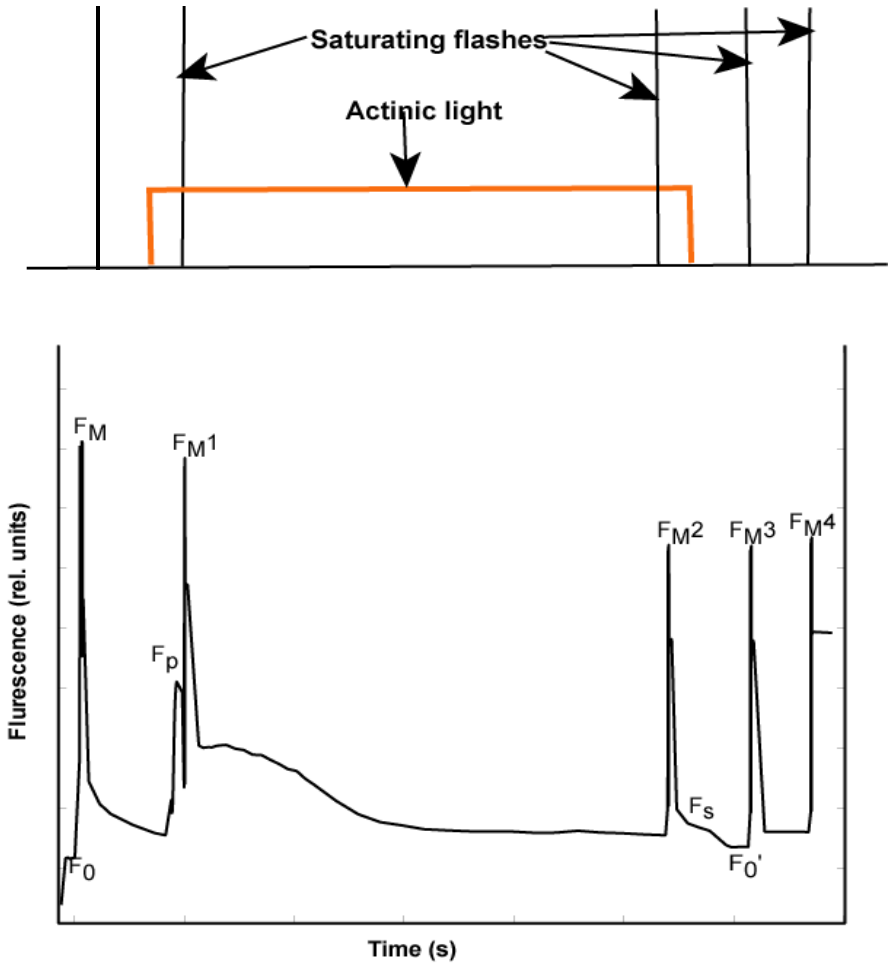

Figure 7. *Experimental protocol for the chlorophyll fluorescence quenching analysis using modulated light. A dark-adapted leaf is exposed to two flashes of saturating light in continuous actinic light and two flashes of saturating light in dark.*

Basic fluorescence parameters

F_0 - minimal fluorescence yield of dark adapted plant with the primary acceptor Q_A oxidized and non-photochemical quenching is inactive

F_0' - minimal fluorescence yield of light adapted plant measured with the primary acceptor Q_A oxidized and non-photochemical quenching active ($F_0' < F_0$)

F_M- maximum fluorescence yield of dark adapted plant exposed to a short pulse of a strong light leading to a transient reduction of Q_A without induction of non-photochemical quenching

F_M'- maximum fluorescence yield of dark adapted plant exposed to a short pulse of a strong light leading to a transcient reduction of Q_A without induction of non-photochemical quenching ($F_M' < F_M$)

F_P- first local maxima of fluorescence yield in presence of actinic light

F_S- steady state fluorescence

Derived fluorescence parameters

F_V= measured in dark adapted plants ($F_{V=} F_M$-F_0)

F_V / F_M – the maximum quantum yield of PSII photochemistry defined as ($F_M - F_0$)/ F_M

Φ_{PSII} – effective quantum yield of PSII photochemistry in light adapted state defined as ($F_M' - F_S$)/ F_M'

qP- photochemical quenching defined as ($F_M' - F_S$) / ($F_M' - F_0'$)

NPQ – non-photochemical quenching calculated as ($F_M - F_M'$)/ F_M'

R_{fd} -fluorescence decrease ratio also called plant vitality index defined as ($F_P - F_S$)/F_S

Apart from fluorescence parameters with physiological significance, some derived fluorescence parameters have no physiological significance, but they may be useful in monitoring related phenomena. For example, the parameter F_0/F_V was used in the study of excitation spectra of PS I and PS II in chloroplasts (Kitajima & Butler 1975) or for the prediction of quality of fruits (Nedbal et al., 2000b).

2. Introduction to advanced statistical tools

2.1 *Pattern recognition*

Pattern recognition is a branch of science dealing with the classification of complex data or objects in different groups (Theodoridis & Koutroumbas 2009). Pattern recognition has been effectively used on microarray based gene – expression data to classify groups of functionally related genes (Hughes et al., 2000) and to forecast broader biological phenotypes such as genetic interactions (Tong et al., 2004), social behavior (Whitfield et al., 2003), character (letter or number) recognition (Yoon 1999, Ren 2000) and used to assist doctors through computer-aided diagnosis for a variety of medical data (Golub et al, 1999). We report a practical application of pattern recognition for the analysis of sequence of chlorophyll fluorescence images in higher plant leaves. We have tried to use classification methods of pattern recognition in order to investigate insight of the complex chlorophyll fluorescence images. Here, in our case, the chlorophyll fluorescence transients (Figure 7, section 1.6) comprising sequence of images are known *pattern* (input data). And each image in the sequence of images is referred as *feature*. FluorCam captures images of chlorophyll fluorescence transients of plants under well defined experimental protocols. Pattern recognition then helps to classify the image into one or two classes (i.e., tolerant/sensitive) using statistical tools of classifiers and feature selection methods.

2.2 *Feature, feature vectors and classifiers*

Abbreviations defining pixels and images

X - *Full dataset: a set of fluorescence transients in all pixels of the camera. From another perspective, it is the image sequence capturing the entire fluorescence transient. The set X consists of real numbers $f_i(t_k)$ that quantify fluorescence emission in the i-th pixel taken at the time t_k during the transient.*

$\boldsymbol{F}_i(t_k)$ - *Fluorescence emission level in the i-th pixel of the k-th image that is recorded at the time t_k. k={1,2…K}; K is the total number of images in the sequence, i.e. number of time points in which the transient is captured, and i={1,2…I}; J is the total number of pixels in each image.*

$\boldsymbol{F}_i$ - *[$f_i(t_1)$, $f_j(t_2)$ … $f_i(t_K)$]: the entire fluorescence transient in the i-th pixel.*

$\boldsymbol{f}(t_k)$ - *k-th fluorescence image in the sequence, i.e., the set of fluorescence levels measured in all pixels at the time t_k.*

As defined above a single image of the fluorescence transient represents a feature and the sequence of all the images measured at different time forms a feature vector.

$$F_i(t_k) = \left[f_1(t_1), f_2(t_2), f_3(t_3), \ldots\ldots\ldots f_I(t_K)\right] \quad \ldots\ldots\ldots\ldots\ldots\ldots\ldots\ldots\ldots\ldots\ldots\ldots\ldots\ldots\ldots\ldots \textbf{(1)}$$

Each of the feature vectors identifies *uniquely a* single pattern (object). The decision rule that ascribes an object to one of the pre-defined classes is called a *classifier*. The role of a classifier is to divide the feature space of corresponding regions, for example, class 1(C_1) and class 2 (C_2). If a feature vector $F_i(t_k)$, corresponding to an unknown pattern, falls in the C_1 region, it is classified as class 1, otherwise as class 2. However, it does not mean that classification decision is correct and misclassifications can be possible. To find correct decision rule one has to utilize information for each point of the known data (class 1 or 2). The feature vectors for which correct classes are known can be used to generate the decision rule (classifier) and are known as *training feature vectors* (Theodoridis & Koutroumbas 2009).

2.3 Supervised and unsupervised pattern recognition

The classification can be divided into two groups know as supervised and unsupervised pattern recognition. For supervised *pattern recognition* a set of training feature vectors are available, and the classifier is designed on the basis of *a priori* known information. However, when the training feature vectors are not available for the given data sets they are classified by unsupervised pattern recognition methods (Theodoridis & Koutroumbas 2009).

2.4 Mean, covariance and covariance matrix

Mean fluorescence transient

The fluorescence transient $\boldsymbol{F}$ averaged over all pixels of the image or of a region of interest is:

$$\boldsymbol{F} = [F(t_1), F(t_2) \ldots F(t_K)], \text{ where } F(t_k) = \langle f_i(t_k) \rangle_{i=1,2..I} \quad \text{..... (2)}$$

Covariance and the covariance matrix

Covariance $Cov(\boldsymbol{f}(t_k), \boldsymbol{f}(t_m))$ is a measure of similarity between two images taken at times t_k and t_m. The offset differences are excluded from the covariance by characterizing each image by the signal deviation from the mean fluorescence signal level, i.e., by $f_j(t_k) - F(t_k)$ and $f_j(t_m) - F(t_m)$ for each pixel j. The covariance $Cov(\boldsymbol{f}(t_k), \boldsymbol{f}(t_m))$ is then calculated as a normalized scalar (or dot) product of the two vectors:

$$\begin{aligned} Cov\big(f(t_k), f(t_m)\big) &= \big(f(t_k)\big) - \big(F(t_k)\big).\big(f(t_m) - F(t_m)\big)/J \\ &= \left\{ \sum_{j=1}^{j,allpixels} \left[\big(f_j(t_k) - F(t_k).\big(f_j(t_m) - F(t_m)\big)\big) \right] \right\} \Big/ J \end{aligned} \quad \text{..... (3)}$$

For $k \neq m$, $Cov(\boldsymbol{f}(t_k), \boldsymbol{f}(t_m)) > 0$ when the deviations from the mean fluorescence signal tend to be parallel in individual pixels of the k-th image (time t_k) and of the m-th image (time t_m): the "high brightness" k-th image segments coincide with the "high brightness" m-th image segments and, at the same time, the "low brightness" k-th image segments coincide with the "low brightness" m-th image segments.

For $k \neq m$, $Cov(\boldsymbol{f}(t_k), \boldsymbol{f}(t_m)) < 0$ when the deviations from the mean fluorescence signal tend to be antiparallel in individual pixels of the k-th image (time t_k) and of the m-th image (time t_m): the "high brightness" k-th image segments coincide with the "low brightness" m-th image segments and *vice versa*.

For two statistically independent images, $Cov(\boldsymbol{f}(t_k), \boldsymbol{f}(t_m)) = 0$. However, $Cov(\boldsymbol{f}(t_k), \boldsymbol{f}(t_m)) = 0$ does not necessarily imply that the two images are completely uncorrelated.

The **covariance matrix** is defined by

$$\sum(\mathrm{X}) = \begin{bmatrix} Cov(f(1), f(1)) & Cov(f(1), f(2)) & \cdots & Cov(f(1), f(K)) \\ Cov(f(2), f(1)) & Cov(f(2), f(2)) & \cdots & Cov(f(2), f(K)) \\ \vdots & \vdots & \vdots & \vdots \\ Cov(f(K), f(1)) & \cdots & \cdots & Cov(f(K), f(K)) \end{bmatrix} \quad \textbf{.....(4)}$$

Size of the matrix is equal to the number of images K. Therefore, the matrix contains covariance between all pairs of images. Diagonal values in the above matrix present the variance of the images. Covariance matrix is often used to show distribution parameters of classes.

2.5 Minimal distance criteria

We can make classification of the images into C classes. An image can be classified as belonging to the class C_i when the class (distribution parameters), class samples, or class mean is defined. Now we will discuss few kinds of distance units that are used in calculating the statistical distances.

2.5.1 Euclidean distance

Euclidean distance E between image $f(t_k)$ and $f(t_m)$ in the D dimensional feature space can be calculated as:

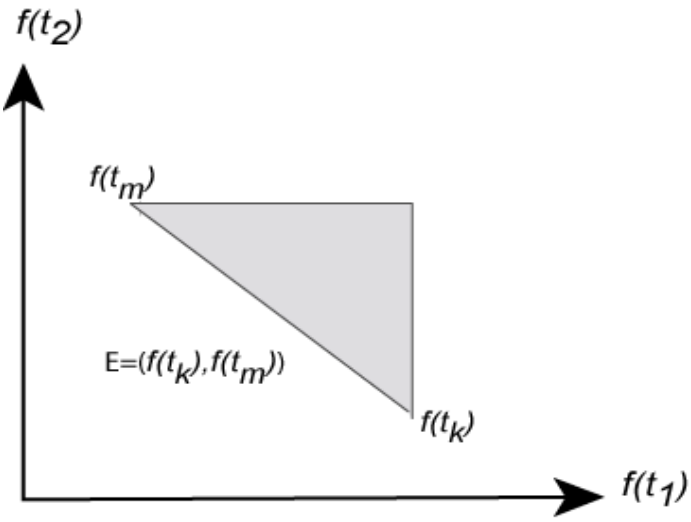

Figure 8. *Euclidean distance between two images $f(t_k)$ and $f(t_m)$ in two dimensional space. Source: Inspired by, http://en.wikipedia.org/wiki/Euclidean_distance*

$$E((f(t_k), f(t_m))) = \sqrt{\sum_{d=1}^{D} (f(t_{kd}) - f(t_{md}))^2} \quad \text{.....(5)}$$

2.5.2 Mahalanobis distance

Mahalanobis distance is constructed to measure distance between the images by taking into consideration of their statistical correlations (Mahalanobis 1930). Squired of Mahalanobis distance is called Mahalanobis squired distance. Let $f(t_k)$ be an image in D dimensional feature space and X set of n images in the same space. Then we can compute the mean vector $<F>$ and covariance matrix of the set X:

$$< F >= \frac{1}{n} \sum_{i=1}^{n} f_i(t_k) \quad \text{..... .(6)}$$

$$\sum X = \frac{1}{n} \sum_{i=1}^{n} (f_i(t_k) - < F >)(f_i(t_k) - < F >)^T \quad \text{.....(7)}$$

$F_i(t_k)$ means fluorescence image captures for i^{th} pixel at k^{th} time of the set X.

Then we can calculate Mahalanobis distance of the image $f(t_k)$ to the image sequence of entire fluorescence transients X:

$$MD = \left(f(t_k) - < F >\right)^T \sum^{-1} \left(f(t_k) - < F >\right) \quad \text{..... (8)}$$

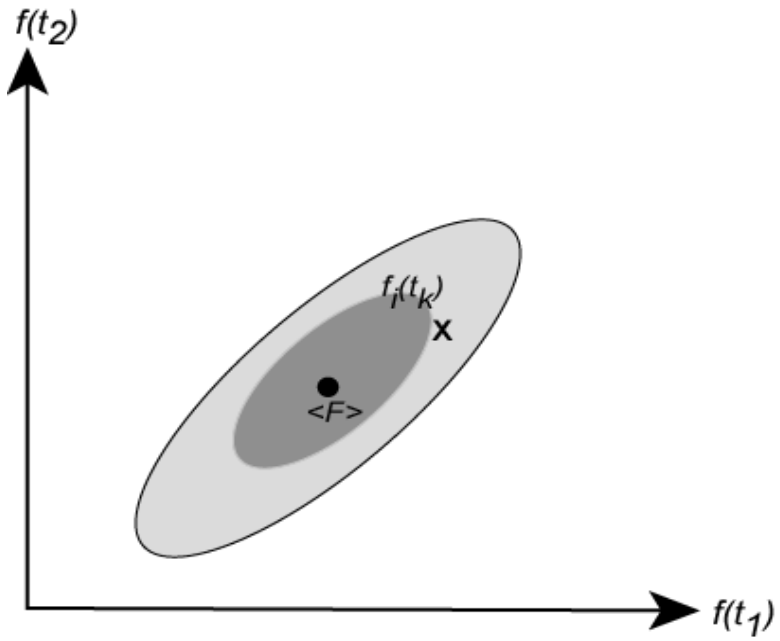

Figure 9. *Dark region shows the area with the same Mahalanobis distance to the full set of X image sequence. This method takes into account the probability properties of the set X. Source: Inspired by, http://www.aiaccess.net/English/Glossaries/GlosMod/e_gm_mahalanobis.htm*

Mahalanobis distance is derived in terms of standard deviation from the center <F> of the set of *X* image sequence. The contour has the form of an ellipse formed around the training data with parameters defined by standard deviation and mean vector of the set *X*. Units of Mahalanobis distance are connected to the probability.

2.5.3 Bhattacharyya distance

Bhattacharyya distance measures distances between two classes by considering overlapping features between them (Bhattacharyya 1943; Bhattacharyya 1946). Bhattacharyya distance

between class C_1 and C_2, defined by *a posteriori* probabilities $p(f_i|\omega_1)$ and $p(f_i|\omega_2)$ (f_i is the fluorescence transient measured for i^{th} pixel), can be computed as:

$$BD(C_1, C_2) = -ln \int_{-\infty}^{\infty} \sqrt{p(f_i \mid C_1)\ p(f_i \mid C_2)}\ d(f_i) \quad \text{..... (9)}$$

When the distribution parameters of classes are identical, the integral will be equal to one and negative logarithm to zero. For classes without the overlap in distributions, the integral is equal to zero and Bhattacharyya distance equal to infinity.

2.6 Classifiers

Classifier is a decision rule that ascribes an object to one of pre-defined classes. Classes are sets of vectors that are similar in one or more features. The classes can be defined in two ways: a) by training set of transients that are selected as a reference to which the classified transients are compared; and b) by quantifying the characteristic features.

a) *Classifier based on training set of vectors that are selected as a reference*

2.6.1 Linear Discriminant Classifier (LDC): LDC makes classification decision rule by using linear combination of features (Fukunaga 1990; Martinez & Kak 2001; Wang & Paliwal 2003). In LDC, each class is characterized by a training set of feature vectors as described in Equation-1. In a simple case, each transient can consist of only two fluorescence parameters, e.g., $f(t_1)$ (=F_0) and $f(t_2)$ (=F_v). Then, the feature space is two-dimensional (K=2) and the separator is a line between the two training classes C_1 and C_2 in Figure 10.

The separating line is calculated from the mean values that is [$<F_0>_{C1}$, $<F_V>_{C1}$] for class C_1, [$<F_0>_{C2}$, $<F_V>_{C2}$] for class C_2 and from the covariance matrices $\sum c_1$ and $\sum c_2$ of both training classes.

For the C_1 class:

$$\sum c_1 = \begin{matrix} c_1(f(t_1), f(t_1)) & c_1(f(t_1), f(t_2)) \\ c_1(f(t_2), f(t_1)) & c_1(f(t_2), f(t_2)) \end{matrix} \quad \text{.....(10)}$$

where,

$$c_1(f(t_1), f(t_1)) = \sum_{i=allC1} (f_i(t_1) - < F_0 >_{c1}).(f_i(t_1) - < F_0 >_{c1})$$

$$c_1(f(t_2), f(t_2)) = \sum_{i=allC1} (f_i(t_2) - < F_v >_{c1}).(f_i(t_2) - < F_v >_{c1})$$

are variances of the constant fluorescence F_0 and of variable fluorescence F_V in the training classC_1.

$$c_1(f(t_1), f(t_2)) = \sum_{i=allC1} (f_i(t_1) - < F_0 >_{C1}).(f_i(t_2) - < F_v >_{C1}) \quad \text{.....(11)}$$

$$c_1(f(t_2), f(t_1)) = \sum_{i=allC1} (f_i(t_2) - < F_v >_{C1}).(f_i(t_1) - < F_0 >_{C1})$$

are the off-diagonal covariances reflecting correlation between the constant and the variable fluorescence signals. Similar covariance is also made for C_2. LDC approaches the problem by assuming that the conditional *probability density functions* $p(f_i(t)|C_1 = 0)$ and $p(f_i(t)|C_2 = 1)$ are both normally distributed with mean and covariance parameters [$<F>_{C1}$, ΣC_1] for C_1 and [$<F>_{C2}$, ΣC_2] for class C_2, respectively. Under this assumption, the Bayes optimal solution predicts the pixels (i^{th}) from the class C_2 if its likelihood ratio is above some threshold T.

$$(f(t) - < F >_{C2}) \sum_{C2}^{-1} (f(t) - < F >_{C2}) + In\left|\sum_{C2}\right| - (f(t) - < F >_{C1}) \sum_{C1}^{-1} (f(t) - < F >_{C1}) + In\left|\sum_{C1}\right| > T \quad \text{.....(12)}$$

Nevertheless, LDC makes an assumption of identical covariance for each class, i.e., $\Sigma_{C1}=\Sigma_{C2}=\Sigma$. The several terms cancel out and the above decision criterion becomes a threshold on the dot product.

$$w.f(t) > T$$

where w is weight vector obtained from covariance matrix, f_i represents i^{th} pixel and T is threshold vector .

for some threshold constant,

$$w = \sum^{-1}(< F >_{C2} - < F >_{C1}) \quad \text{..... (13)}$$

And the linear combinations for the separating line can be written as:

$$L(f_i) = w^T(f_i) + T \quad \text{.....(14)}$$

The decision rule for the two classes is defined as:

$$if \begin{cases} L(f_i) > 0, & \text{corresponding pixel belongs to } C_2 \\ otherwise, & C_1 \end{cases} \quad \text{..... (15)}$$

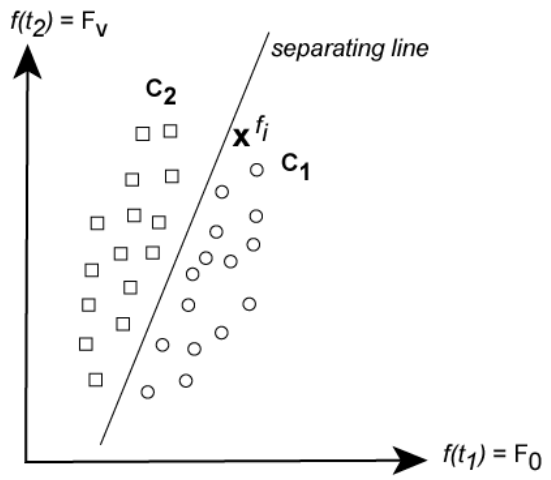

Figure 10. *Linear Discriminant Classifier (LDC) in a 2-dimensional feature space. The training class C_1 is characterized by a low F_0 (=$f(t_1)$) and a high F_V (=$f(t_2)$), e.g., in pixels capturing emission from photosynthetically active leaf regions. The training class C_2 represents pixels of less photosynthetically active regions. Source: Theodoridis & Koutroumbas 2009*

2.6.2 Fisher's Linear Discriminant Classifier (FLDC): There is a slight difference in discrimination process between FLDC (Fisher 1936) and LDC that is the process to obtain the separating line. To construct the separating line, FLDC does not make an assumption of identical class covariance. In FLDC, separating line maximizes the distance between the means of the two classes while minimizing the covariance within each class. Fisher's linear discriminant function can be written in a similar to Equation 14. However, weight vector *w* can be calculated as :

$$w = \frac{\left| < F >_{C1} - < F >_{C2} \right|^2}{\sum_{C1} + \sum_{C2}} \quad \textbf{.....(16)}$$

Where $<F>_{C1}$ is the mean vector of 1^{st} class and Σ_{C1} *is the* covariance matrix of this set (similar for$<F>_{C2}$). The decision rule for the two classes is defined as:

$$if \begin{cases} L(f_i) > 0, & corresponding\ \ pixel\ belongs\ to\ C_2 \\ otherwise, & C_1 \end{cases}$$

2.6.3 Quadratic Discriminant Classifier (QDC): QDC uses quadratic discriminant functions to find the separating line between the two classes (Pekalska &Duin 2001; Paclik & Duin 2003). Unlike LDC, no assumption is made about identical covariance for each class in constructing separating line in QDC.

If the covariance matrix of the two classes is identical, they can be linearly separated and QDC finds the parameters for the separating line which is linear in this case. Therefore, QDC and LDC will have identical function. If covariance matrices are different, separating line is quadratic. The unbiasedness of this classifier assures good estimation with large amount of data. In case of the QDC, when the mean and covariance of each class is known the likelihood ratio will be

$$\frac{\sqrt{2\pi|\Sigma_{C2}}^{-1}\, \boldsymbol{exp}\left(-\frac{1}{2}(f(t)-<F>_{C2})^T \Sigma_{C2}^{-1}(f(t)-<F>_{C2})\right)}{\sqrt{2\pi|\Sigma_{C1}}^{-1}\, \boldsymbol{exp}\left(-\frac{1}{2}(f(t)-<F>_{C1})^T \Sigma_{C1}^{-1}(f(t)-<F>_{C2})\right)} < T \quad \textbf{.....(17)}$$

For the threshold *T,* and the resulting separating surface between the classes will be quadratic.

The decision rule for the two classes is defined as:

$$if \begin{cases} Q(f_i) > 0, & corresponding\ \ pixel\ belongs\ to\ C_2 \\ otherwise, & C_1 \end{cases}$$

In Figure 11, the classified pixel f_i is the member of class C_1 because the covariance matrix for the two classes are different and using quadratic separating line it is found to be on the same side of the separating line as class C_1.

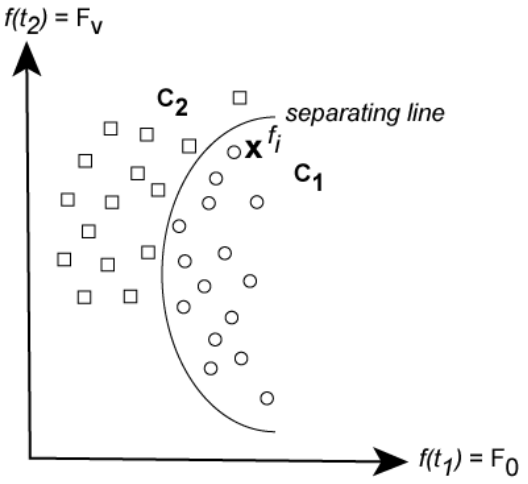

Figure 11. *Quadratic Discriminant Classifier (QDC) in a 2-dimensional feature space. In QDC, covariance matrixes are different, and the separating line is shown quadratic. Source: Inspired by, http://cmp.felk.cvut.cz/cmp/courses/recognition/Labs/perceptron/index_en.html*

***2.6.4 Support Vector Classifier (SVC)*:** A support vector machine constructs a separating line or set of separating lines in an infinite dimensional space, which can be used for classification (Boser et al. 1992; Brown et al. 1999; Camps-Valls et al. 2004). The best separation is achieved by the line that has the largest distance to the nearest training data points of any class (margin), since larger the margin the lower will be error of the classifier.

$$S(f_i) = w^T f_i + T \quad \text{.....(18)}$$

Here, w is weight vector obtained by covariance matrix, f_i represents the i^{th} pixel and T is the threshold vector. Every separating line is characterized by its direction (determined by w) and its exact position in the space (determined by T). Since we want to give no preference to either of the classes, then it is reasonable for each direction to select that separating line which has the same distance from the respective nearest points in C_1 and C_2 (Fig. 12). Our goal is to search for the direction that gives the maximum possible margin.

$$z = \frac{|S(f_i)|}{\|w\|} \quad \text{-..... (19)}$$

The nearest points in C_1 and C_2 (Fig. 12) is equal to 1 for C_2 and equal to –1 for C_1. This will be equivalent with having a margin of

$$\frac{1}{|w|} + \frac{1}{|w|} = \frac{2}{|w|} \quad \text{.....(20)}$$

$$if \begin{cases} S(f_i) > 0, & corresponding\ \ pixel\ belongs\ to\ C_2 \\ otherwise, & C_1 \end{cases}$$

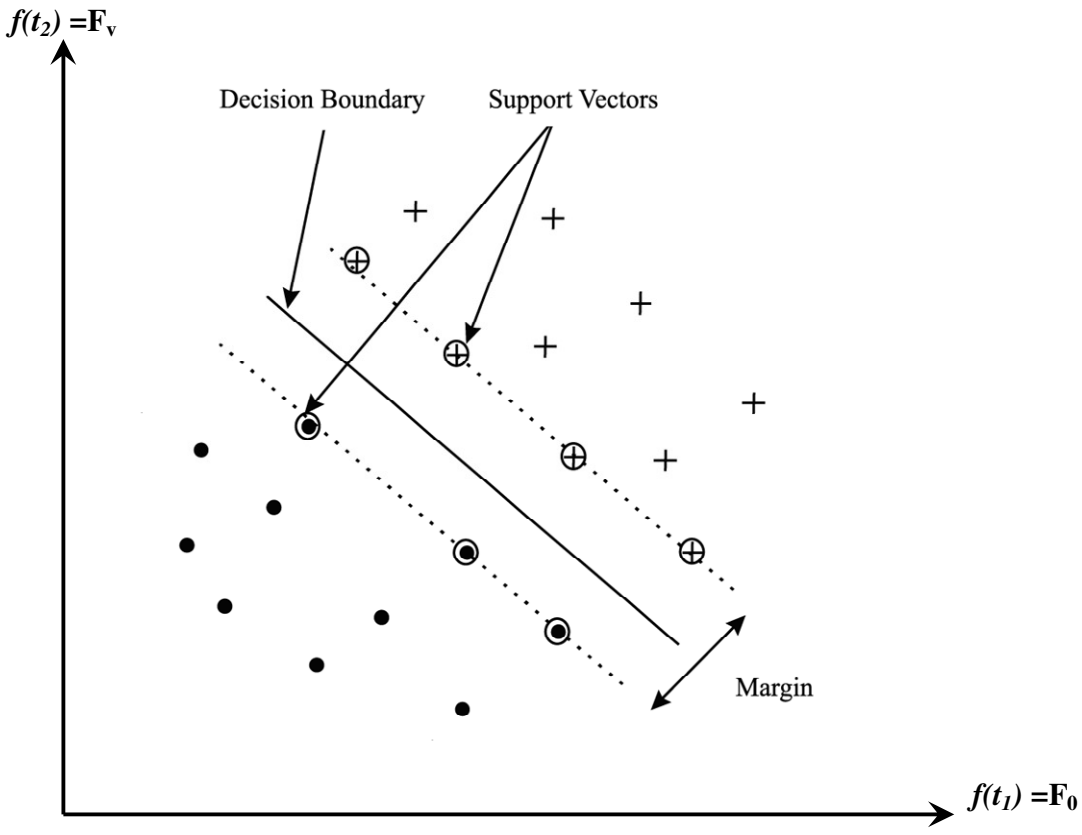

Figure 12. *The Support Vector Classifier (SVC) in a 2-dimensional feature space. The decision boundary separates the two classes by maximizing the margin. The separating line shown with dark lines and the margin is indicated by dotted lines. Our goal is to search the separating line that gives the maximum possible margin.*
Source: Inspired by,
http://www.emeraldinsight.com/journals.htm?articleid=870666&show=html

b) Classifier based on characteristic features

***2.6.5 Nearest Neighbor Classifier (NNC)*:** NN classifier (Fukunaga & Hostetler 1975) calculates the Euclidian distances (ED, see Figure13) between pixel f_i to all pixels in the training set for each class. This method compares the distance and finds the pixel at the

closest distance and classifies f_i to the same class of the closest pixel. In the figure, f_i is a member of class C_2 based on its nearest neighbor.

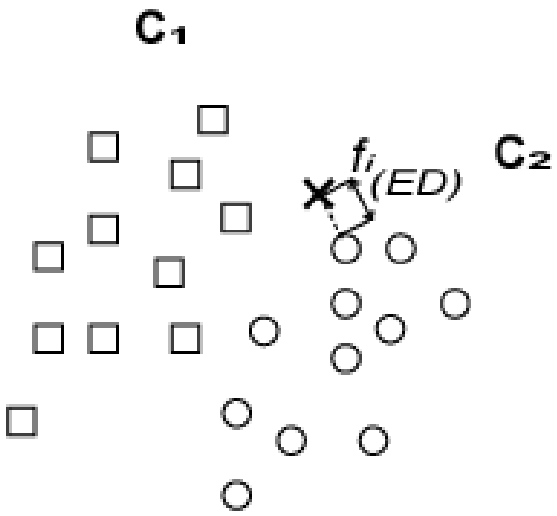

Figure 13. *The Nearest Neighbor Classifier* ***(NNC)*** *in a 2-dimensional feature space. The pixel is found to be closest to the class C_2 and classified as a member of class C_2 after comparing its distance (Euclidian Distance, ED) to the training set (reference) for both classes. Source: Inspired by,http://www.springerimages.com/Images/LifeSciences/5-10.1186_1471-2105-7-73-3*

2.6.6 k-Nearest Neighbor Classifier (k-NNC): The function of the *k*-NN classifier (Fukunaga & Hostetler 1975) is very close to that of the NN classifier. Euclidian distance of pixel f_i is calculated for all the pixels of the training set. Finally, this classifier finds the k (k=3) nearest neighbors and puts f_i to the class that has the highest number of nearest neighbors. In the figure 15 (using *k*-NN classifier with $k = 3$), f_i is classifed as a member of the class C_2 as it contains two nearest neighbors from this class.

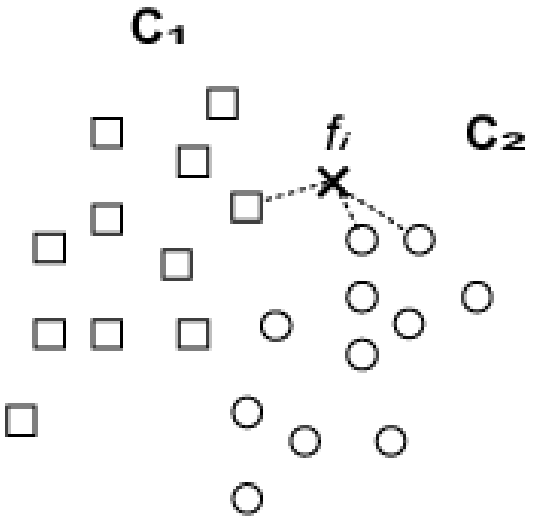

Figure 14. *The k-Nearest Neighbor Classifier (k-NNC) in a 2-dimensional feature space. The distance (Euclidian Distance, ED) of f_i is compared with the 3(k=3) closest neighbors and classified as a member of class C_2 on the basis of large number of close neighbors. Source: Inspired by, http://www.springerimages.com/Images/LifeSciences/5-10.1186_1471-2105-7-73-3*

***2.6.7 Nearest Mean Classifier (NMC)*:** NMC (McQueen 1967) characterizes the classes by their corresponding mean vectors (presented with dark color in Figure 15). It classifies pixel f_i to the nearest class on the basis of the minimal distance between f_i and the mean vector of that class. In the figure, f_i is classified as a member of class C_1 because it is nearer to the mean vector of the class C_1.

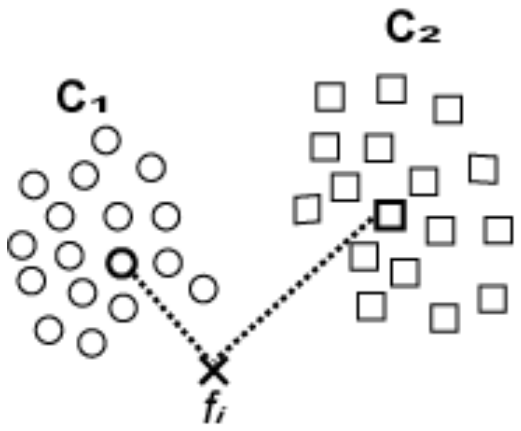

Figure 15. *The Nearest Mean Classifier (NMC) in a 2-dimensional feature space. The pixel is found to be closest to the class C_1 and classified as a member of class C_1 after comparing its distance (Euclidian Distance, ED) to mean (centroid) of both classes. Source: Inspired by,http://zone.ni.com/reference/enXX/help/372916H01/nivisionconcepts/classification_methods/*

2.7 Feature extraction and feature selection

Multidimensional space (D) generally contains large number of vectors and for the classification purposes many elements of the vectors can be unnecessary. There are two major reasons for which the dimension of the measured vectors cannot be taken to be too large for classification (Heijden et al., 2004).

i. Large data sets increase the computational complexity. For example a linear classification having C number of classes and D dimensions needs $C*D$ operations, while a quadratic classification requires $C*D^2$ operations. However the memory requirement for binary measurements is in the order of $C2^D$ for quadratic classification.
ii. Increase in dimensions causes a decrease in the performance of classification.

There can be two strategies of classifications of multidimensional data sets. First, by the use of appropriate classifiers or discrimination functions that requires prior knowledge of data

sets and may automatically reduce wrong classifications. The second strategy employs reduction of the dimensions of input data set. For the dimensionality reduction, there exist two approaches known as ***feature selection*** and ***feature extraction. Feature selection*** methods eliminate redundant elements of the vector and process remaining useful data. While in ***feature extraction*** methods the input data set is transformed into reduced features vectors and the most relevant information is extracted using reduced data rather than using full size input data set.

2.7.1 Feature selection

Feature selection techniques are used to identify subsets of images that carry relevant information to maximize the contrast between classes. Such a unique subset is called feature set and its elements are features. This can be written in the form of following equation also described in Heijden et al., (2004).

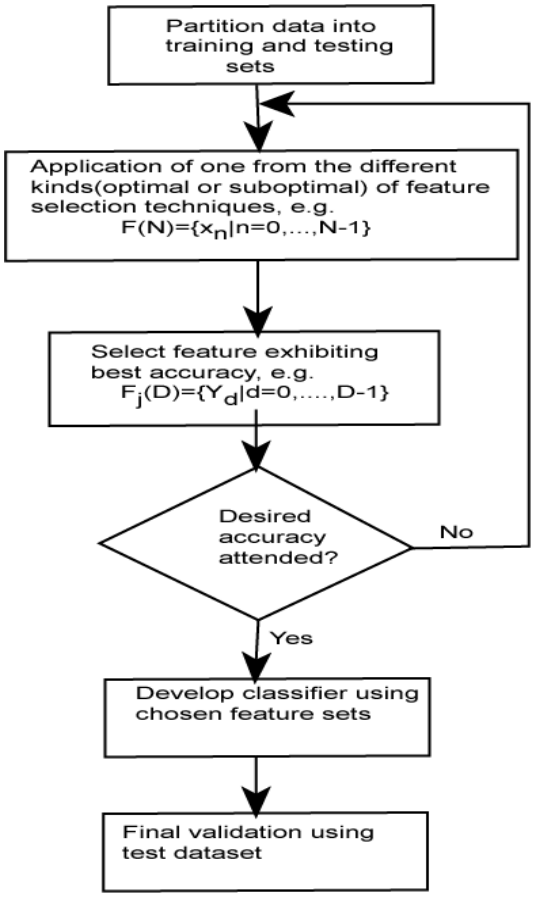

Figure 16. *The feature selection approach where the feature subset is generated by iterative evaluation of available feature flow chart.*

$$F(N)=\{x_n|n=0,...,N-1\} \quad \text{.....} \quad \textbf{(21)}$$

where x_n is a feature belonging from n=1 to *N-1* from the measured feature vector x. Let us assume that $F_j(D)=\{y_d|d=0,....,D-1\}$ be a subset of $F(N)$ consisting of $D < N$ elements taken from feature vector x. And j= *1,2,….q(D),* where *q(D)* is total number of possible subsets of *F(N)*. For each elements of subset $F_j(D)$ there exists an element *on F(N)* such that $y_d = x_n$.

Thus, number of subsets for a given D can be formulated as:

$$q(D) = \binom{N}{D} = \frac{N!}{(N-D)!\,D!} \quad \text{..... (22)}$$

In the above **equation- 22**, *q(D)* shows all the distinguishable subsets that can be made from *N* elements of data sets, where each subset contains *D* elements but none of them have the identical elements.

Figure 16 shows a flow chart describing the steps to find the best subset from the huge combination of possible subsets. The feature selection algorithm selects one subset and enquires if the required accuracy has been obtained or not. If not it goes back and select other subset and continue the iterations until it finds the best subset. Thus, highly informative subset selected by feature selection algorithm is used to develop the appropriate classifier to solve the given task.

Feature selection needs an exhaustive search to find the best subset out of $q(D)$ subsets. For example, if we put N=20 and D =10 in above equation, it gives about 1.85×10^5 different combination of subsets. Therefore, selection of the best subset out of these huge combinations is much more complicated.

In order to overcome the complexity of selection of best subsets we need an efficient search strategy. There exist optimal methods and sub-optimal methods for this purpose. Optimal methods such as ***'Branch and bound'*** can guarantee for the best subset selection but they require huge computational time. However, suboptimal methods such as ***Individual Feature Selection (IFS), Sequential Forward Selection (SFS), Sequential Backward Selection (SBS)*** and ***Sequential Forward Floating Selection (SFFS)*** methods do not guarantee if the subset with the best performance is selected but are comparatively faster than optimal methods. Out of all available methods based on optimal and suboptimal methods we have selected suboptimal methods for our analysis. This method gives us reasonably better subset in less computational time.

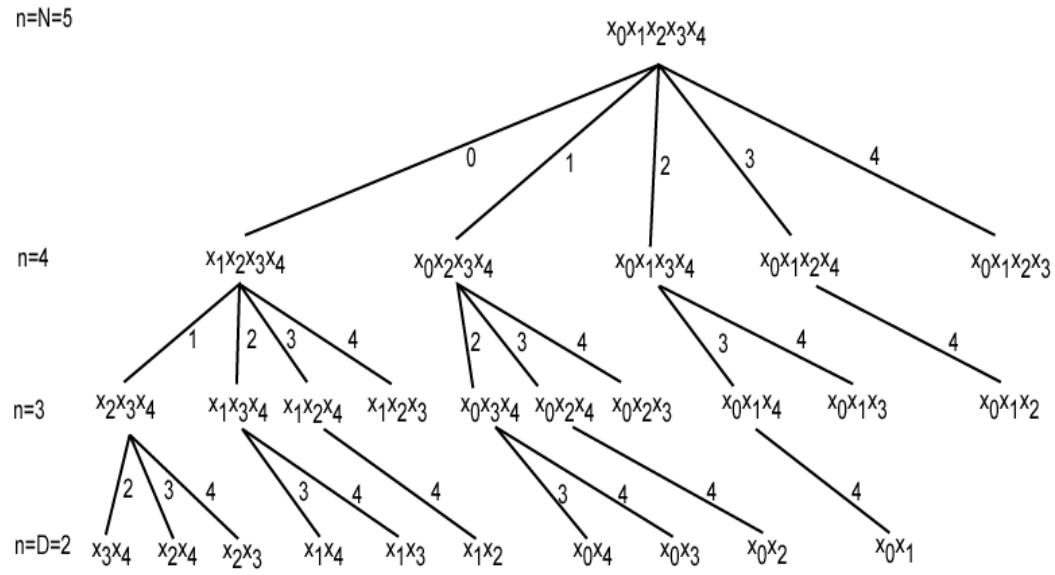

Figure 17. *The top down tree using 'branch and bound' feature selection method which guarantees the best performing subset using optimal strategy of feature selection. Source: Heijden et al., 2004.*

2.7.2 Branch and bound feature selection technique (optimal method)

The ***branch and bound*** method works similar to that of a tree structure as shown in Figure 17. In fact, it measures the performance of subset at different branch levels in the tree structure with increasing dimensions *D* (Heijden et al., 2004). For example, if we select *N*=5 it can have *N*-*D*+1 branch levels, where minimum value of *D* is the least number of elements (n=*D*=2) in the possible subsets. The search process starts with measurement of performance of subset at highest branch level ($n = N$). Subsequently, it measures the performance of other subsets until the lowest branch level (n=D) and select the best performing subset of the tree. Therefore, relative to exhaustive search, this algorithm is much more computationally efficient.

The main idea of branch and bound methods is to compare a node's bound value of a branch level with the best subset on it. If the performance of the subsequent node's bound is not

better than previously found subset, then the node is accepted as useless and its associated subsets are terminated from further analysis because no solution obtained from that node can be better than the best subset found.

There are certain limitation of ***branch and bound*** algorithm:
Even branch and bound method is better then the exhaustive search, it requires too much computational time. Other disadvantage of branch and bound method is its top-down search strategy, which starts with full set of data and deleting the elements as it progress and ultimately finds the best performing subset. In practice down-top search is more preferable to avoid overoptimistic view which may happens when the number of measurements is too large.

2.7.3 Suboptimal feature selection methods

i Individual Feature Selection (IFS). This method calculates the performance of every single image and sorts them according to their performance. In this way, it uses n single best images to make a subset of the best images, where n is defined by the user. This method for feature selection is least time consuming because the number of calculating performances is equal to the number of images. However, it has poor performance because the subset of n single best images is different than the best subset of images.

ii Sequential Forward Selection (SFS). This method starts searching for the best image in the whole image sequence and puts it inside the empty subset (Kittler, 1978). Then, it starts searching the best image* in the rest of image sequence and puts it again inside the same subset. This method of adding best image is continued until the required numbers of images are obtained.

iii Sequential Forward Floating Selection (SFFS). This method works in a similar way as the SFS (Pudil et al., 1994). However, after every addition it allows removal of the least performing image from the newly formed image subset for achieving higher performance.

* Best image-the image that contributes to performance of image subset with highest increment.

Thus, it might be possible that the addition of single best performing image reduces the performance when it performs in the subset. It finally stops after getting the required number of images in the subset.

iv Sequential Backward Selection (SBS).This method (Kittler 1978) starts with the subset containing all the images. At every step it search for the least performing image and removes it from the subset. It stops after getting the subset with required number of images.

3. Material and Methods

3.1 *Plant material*

The detailed description of the plant material, used for this research, is given in Chapter 4 of this thesis, and in the accompanying publications (Mishra et al., 2009; A. Mishra et al., 2011 and K.B. Mishra et al., 2011). In short, we have worked with basil (*Ocimum basillicum*), oregano (*Origanum vulgare*) and sweet marjoram (*Origanum majorana*) - of the family *Lamiaceae;* for the species discrimination experiment, see chapter 4.1. In chapter 4.2, we have used a collection of nine natural accessions of *Arabidopsis thaliana* originating from a very warm climate in Portugal to a very cold climate in Finland; these were used to study their cold tolerance. The cold tolerance was quantified by the well established electrolyte leakage method on the detached leaves and chlorophyll fluorescence transients were measured during constant cooling to subzero temperatures to reveal plant tolerance to low temperatures. In chapter 4.3, we have used the wild type and drought tolerant transgenic tomato line DTL-20, carrying *ATHB*-7 gene, to investigate the potential of chlorophyll fluorescence to report drought tolerance under well irrigated and water limited conditions.

3.2 *Fluorescence imaging systems*

3.2.1. Kinetic imaging FluorCams

Kinetic imaging FluorCams are imaging fluorometers that measure sequences of Chl-fluorescence images with user-defined irradiance and timing protocols. Fluorescence emission is induced by two (or more) panels of light emitting diodes (LEDs) that provide measuring flashes. The FluorCam is equipped with a CCD camera (512 x 512 pixels, 12 bits) and two (or more) light emitting diode panels, as described in Nedbal et al.,(2000a). Photochemistry is driven by continuous actinic irradiance and by strong saturating pulses of light that are generated by a halogen lamp, equipped with a shutter, or by supplemental LEDs. In the new version of FluorCam, LEDs are also used to generate saturating pulses.

Flashes of the LEDs were synchronized with the opening of the electronic shutter of the CCD camera. The camera allows imaging of fluorescence transients that are induced by actinic light or by saturating flashes. An optical filter RG695 (Schott) was placed in front of the CCD camera to block the exciting light and allow recording of fluorescence images in the 700-750 nm region. The timing and amplitude of actinic irradiance are determined by user-defined protocols. Data are transmitted via a USB 2.0 port to a desktop computer or to a notebook.

FluorCam captures the kinetics of Chl *a* fluorescence by using existing experimental protocols such as quenching protocol and it has the flexibility to generate our own experimental protocol of interest. A software integrated with FluorCam software can be used either to visualize single images or fluorescence parameters of interest. We can use it to detect the dynamics and the spatial heterogeneity in various fluorescence parameters of physiological significance. And also, if needed, we can determine the numeric value of the chlorophyll fluorescence parameters from the measured chlorophyll fluorescence images.

We have used following versions of FluorCam to obtain the data of our experiments.

Open version of FluorCam (Fig. 18, Photon Systems Instruments, spol. s. r. o., Brno, Czech Republic, *www.psi.cz*). Chlorophyll fluorescence was excited with short (10–30 μs) measuring flashes and photochemistry was elicited by actinic light from the same set of orange Light Emitting Diodes (LED, 620nm). Saturating flashes were provided by a halogen lamp. The flashes were synchronized with the opening of the electronic shutter of the CCD camera (512 x 512 pixels, 12 bits) capturing the ChlF images. An optical filter RG695 was placed in front of the CCD camera that blocked the exciting light and allowed the measurement of the ChlF transient in the 700-750 nm range.

Figure 18. *Photograph of open version of FluorCam.*

Handy FluorCam (Fig. 19, The FC 1000-H). It has been designed to measure kinetically resolved fluorescence images of leaves and of small plants (smaller than 3 x 3 cm). The FC 1000-H was equipped with a four orange light emitting diode panels (wavelength, 620 nm, panel size 40x40 mm, each panel containing 25 LEDs). The four LED panels can be used to generate short measuring flashes (10–250 µs), continuous actinic light as well as saturating flashes with adjustable in duration and power (upto 2,000 µmol (photons) $m^{-2}s^{-1}$)).

Figure 19. *Photograph of Handy FluorCam.*

3.2.2. Software for image analysis

All calculations and analysis were carried out in MATLAB 6.5. For the statistical pattern recognition, we used Pattern Recognition Toolbox PRTools v. 3.0, which is freely available for non-commercial and academic purpose (*http://www.prtools.org/*). Algorithms of this toolbox randomly divide the data (vector of fluorescence transients in individual pixels) in two parts for the pattern recognition. One part is used as a reference to characterize the classes and the other part is used for simulated classification that serves to assess the algorithm performance. Programs were run on computer with AMD Athlon 64 3000 (2.60GHz, 512 KB cache) with 1.25 GB of RAM. The operating system was Windows XP, Version 2002. GraphPad Prism (*http://www.graphpad.com*, CA, USA), was used for basic biostatistics, curve fitting.

3.3 Measuring protocols

Chlorophyll fluorescence transients were captured using FluorCam devices mentioned above. The output of such measurement is a sequence of fluorescence images over time. Standard quenching (described in Fig 20) or a complex quenching experimental protocol was used to measure chlorophyll fluorescence transients.

Complex quenching protocol

The physiological state of a plant is typically assayed by measuring the temporal changes in chlorophyll fluorescence yield by using the well known standard quenching protocols (Schreiber et al., 1986; see Figure 20). In addition to standard quenching protocols, we have used the so-called complex quenching protocol that uses combination of two standard quenching protocols with varying actinic light intensity. The exact measuring protocols, used for the experiments, are given in the respective chapters. However, here, we present a general description of the complex protocol shown in Figure 20.

The protocol starts by exposing a dark-adapted plant to actinic light of 50 and 200 µmol (photons) $m^{-2}s^{-1}$ for 70 seconds, respectively, with a 600 s gap between them. The actinic light leads to partial and transient congestion of photosynthetic electron transport chain. Two

saturating flashes in continuous actinic light allows the measurement of NPQ (non photochemical quenching of the excited state of Chl a) and a short dark adaptation followed by two other saturating flashes after switching off the actinic light allows the measurement of NPQ recovery (Horton & Ruban 1992). Nine saturating light flashes were applied in this complex protocol to probe photochemical and non-photochemical quenching mechanisms. The saturating flashes and actinic light leads to a complex fluorescence transient.

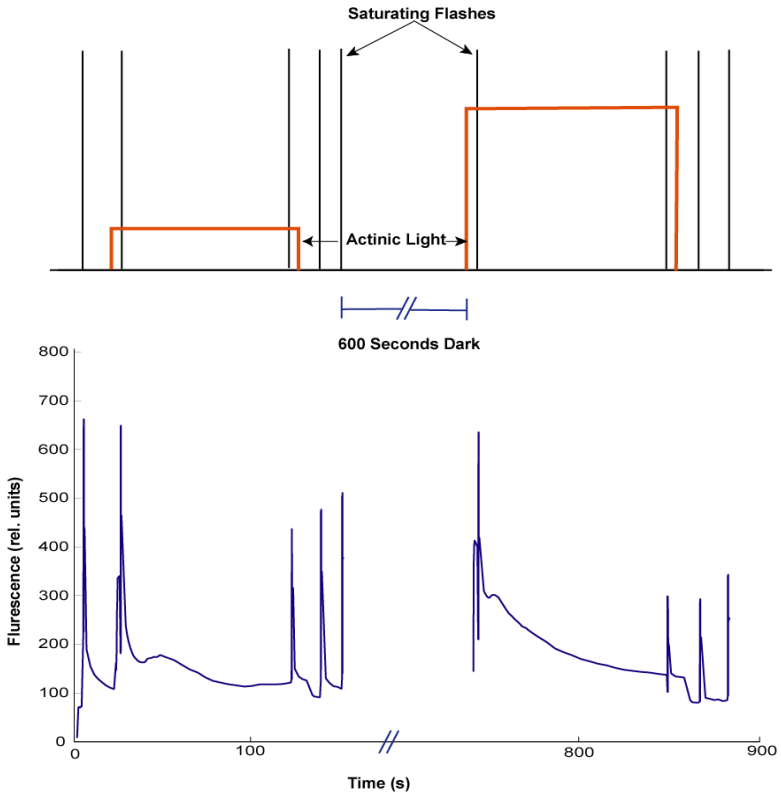

Figure 20. *The complex protocol for chlorophyll fluorescence quenching analysis containing two levels of actinic light with a gap of 600 s during the measurement.*

3.4 Selection criteria of statistical methods for the feature recognition

The approach chosen for the recognition of each class depends on the selection of a suitable classification method, its setting and the selection of feature selection method to find the most informative images from the sequence of images captured by imaging FluorCam.

The ChlF transients recorded are used for training and evaluating the performance of the classifiers. Basically each class is represented by a huge number of transients captured in different pixels, representing different leaves and individual plants and taken at different times. Out of this enormous data set, we select at random ~ 4000 to 6000 transients for each class. Thus, selected sets of transients represent transients of different classes. After that, we randomly and evenly divide them into two pixel subsets each for the training and testing of each class. The training sets are used as a reference to represent the classes, whereas the mixed testing set is used to evaluate the performance of individual classifiers. Transients arbitrarily chosen from the testing set are compared with each of the training sets and classified as belonging to one of class using the classifier algorithm (explained in 2.6). The classification is then validated to be either true or false by confronting the classification result with the origin of the particular transient in particular class. The performance of each of the investigated classifiers is quantified by a number between 0–1: value '0' meaning random classification and value '1' meaning that the classifier is 100% successful. For selecting the best classifier the computation time is another important factor to be considered; finally, we choose the best performing classifier on the basis of its performance and the least computational time.

The ChlF transients were captured in extensive series of fluorescence images, called features in our study. Feature selection algorithms (explained in section 2.7) are designed to reduce the number of features (fluorescence images) for an effective classification. The reduction is based on an identification of an image sub-set that contains the most useful information for the discrimination between the classes.

4. Results and Discussions

4.1 Towards discrimination of plant species by machine vision: advanced statistical analysis of chlorophyll fluorescence transients

Journal of Fluorescence, 2009

Anamika Mishra, Karel Matouš, Kumud B. Mishra and Ladislav Nedbal

Abstract

Automatic discrimination of plant species is required for precision farming and for advanced environmental protection. For this task, reflected sunlight has already been tested whereas fluorescence emission has been only scarcely considered. Here, we investigated the discriminative potential of chlorophyll fluorescence imaging in a case study using three closely related plant species of the family *Lamiaceae*. We compared discriminative potential of eight classifiers and four feature selection methods to identify the fluorescence parameters that can yield the highest contrast between the species. Three plant species: *Ocimum basilicum, Origanum majorana* and *Origanum vulgare* were grown separately as well as in pots where all three species were mixed. First, eight statistical classifiers were applied and tested in simulated species discrimination. The performance of the Quadratic Discriminant Classifier was found to be the most efficient. This classifier was further applied in combination with four different methods of feature selection. The Sequential Forward Floating Selection was found as the most efficient method for selecting the best performing subset of fluorescence images. The ability of the combinatorial statistical techniques for

discriminating the species was also compared to the resolving power of conventional fluorescence parameters and found to be more efficient.

J Fluoresc
DOI 10.1007/s10895-009-0491-x

ORIGINAL PAPER

Towards Discrimination of Plant Species by Machine Vision: Advanced Statistical Analysis of Chlorophyll Fluorescence Transients

Anamika Mishra · Karel Matouš · Kumud B. Mishra · Ladislav Nedbal

Received: 1 November 2008 / Accepted: 1 May 2009

Abstract Automatic discrimination of plant species is required for precision farming and for advanced environmental protection. For this task, reflected sunlight has already been tested whereas fluorescence emission has been only scarcely considered. Here, we investigated the discriminative potential of chlorophyll fluorescence imaging in a case study using three closely related plant species of the family *Lamiaceae*. We compared discriminative potential of eight classifiers and four feature selection methods to identify the fluorescence parameters that can yield the highest contrast between the species. Three plant species: *Ocimum basilicum, Origanum majorana* and *Origanum vulgare* were grown separately as well as in pots where all three species were mixed. First, eight statistical classifiers were applied and tested in simulated species discrimination. The performance of the Quadratic Discriminant Classifier was found to be the most efficient. This classifier was further applied in combination with four different methods of feature selection. The Sequential Forward Floating Selection was found as the most efficient method for selecting the best performing subset of fluorescence images. The ability of the combinatorial statistical techniques for discriminating the species was also compared to the resolving power of conventional fluorescence parameters and found to be more efficient.

A. Mishra (✉) · K. Matouš · K. B. Mishra · L. Nedbal
Institute of Physical Biology, University of South Bohemia,
Zámek 136,
37333 Nové Hrady, Czech Republic
e-mail: amishra@greentech.cz

A. Mishra · K. Matouš · K. B. Mishra · L. Nedbal
Institute of Systems Biology and Ecology,
Academy of Sciences of the Czech Republic,
Zámek 136,
37333 Nové Hrady, Czech Republic

Published online: 16 May 2009

Keywords Classification · Feature selectionl · Chlorophyll fluorescence transient · Precision farming · Statistical classifier

Acronyms and symbols

CCD	Charge Coupled Device
ChlF	Chlorophyll Fluorescence
F_0	minimal fluorescence level of dark adapted plants when primary quinone accepter (Q_A) of Photosystem II is oxidized
F_M	maximal fluorescence level of dark adapted leaves measured when Q_A and the plastoquinone pool are reduced
$F_V=F_M-F_0$	variable fluorescence
FLDC	Fisher's Linear Discriminant Classifier
IFS	Individual Feature Selection
k-NN	*k*-Nearest Neighbor Classifier
LDC	Linear Discriminant Classifier
NEURC	Automatic neural networks Classifier
NMC	Nearest Mean Classifier
NN	Nearest Neighbor Classifier
NPQ	Non-Photochemical Quenching
QDC	Quadratic Discriminant Classifier
qP	Photochemical quenching
Rfd	Fluorescence decrease ratio
SBS	Sequential Backward Selection
SFFS	Sequential Forward Floating Selection
SFS	Sequential Forward Selection
SVC	Support Vector Classifier

Introduction

Species discrimination is applied in precision farming for machine weeding or to reduce excess use of agrochemicals

by a targeted application [1, 2]. Weed detection in crop fields and a targeted application of agrochemicals can save 50–90% of herbicides. Such a reduction would lead to significant economic and ecologic benefits [1, 3, 4]. Several methods based on machine vision of reflected natural light are available for the discrimination of plant species in field [5–7]. One class of techniques discriminates the species using their shape, size, and image texture [8, 9]. These techniques have several limitations, e.g., due to shapes that vary greatly with viewing angle, overlapping leaves that are hard to resolve, and segmentation that can be difficult due to non-uniform illumination [10]. The main disadvantage of shape-based techniques is low performance in real time [11].

Other methods utilize differences in the spectrum of the light that is reflected from plants. Earlier, the spectral resolution was limited by use of a multispectral reflectance sensor that measured the reflectance images only within several wide spectral bands [12]. With such a limited spectral resolution, non-uniform light illumination that often occurs in field conditions can greatly complicate species discrimination [13, 14]. Later, hyperspectral reflectance sensors were developed that measure hundreds of images, each in a very narrow band of the reflected light. However, the classification accuracy remained frequently inadequate even with the hyperspectral resolution (see [15], reviewed in [16]).

Rather than using reflected light, we focus here on actively excited chlorophyll fluorescence (ChlF) emission, the reporter signal that has already proven its potential both in research and in numerous applications [17, 18]. The imaging variant of the technique measures hundreds of ChlF images capturing fluorescence transient that occurs in response to actinic light exposure [18]. Many conventional ChlF parameters have been identified that have physiological interpretation and are useful for, e.g., assessment of plant health status and early detection of biotic and abiotic stresses [19–21]. We suggest that the information in the ChlF transients can be also used for plant species identification [22, 23].

Practical application of the species discrimination based on hyperspectral reflectance or on fluorescence emission imaging is limited by potentially long time intervals that may be required to collect and analyze data in real time [22, 24, 25]. The long acquisition time required to capture some of the conventional fluorescence parameters (e.g., NPQ or Rfd), [26] must be solved by development of alternative experimental protocols and/or by use of ChlF parameters that can be acquired in real time and fast enough for the particular application.

In the present work, we focus at the computation time that can be reduced by eliminating redundant or low-contrast information and by selective use of information-rich images as identified by feature selection methods [27, 28] or by genetic algorithms [23, 29, 30]. Recently, we applied a combination of the *k*-Nearest-Neighbor (*k*-NN) classifier and the Sequential Forward Floating Selection (SFFS) feature selection method to discriminate infected and non-infected segments of leaves of *Arabidopsis thaliana* [27, 28]—a task homologous to species discrimination. Here, we aim at finding the best performing statistical methods that are selected from a broader spectrum of classifiers and feature selection methods. The contrasting features found by this optimized technique are compared with discrimination performance of the conventional ChlF parameters as they are presently used in plant science.

Material and methods

Plant material and growth conditions

Three closely related species: basil (*Ocimum basilicum)*, oregano (*Origanum vulgare*) and sweet marjoram (*Origanum majorana*), all of the family *Lamiaceae*, were selected for the experiment. The seeds of these plants were germinated in pots of 0.08 m diameter containing garden soil at room temperature, under natural relative humidity and light regime at the window of our laboratory. 30–50 plantlets of given species grew in each pot. In another set-up, seeds of the three species were randomly mixed (3×10–20 seeds of each) and germinated in three pots. The ChlF transients were measured 10 days after germination.

Chlorophyll fluorescence imaging

The sequences of ChlF images were measured using open version of FluorCam (Photon Systems Instruments Ltd.), Brno, Czech Republic, [31]. The plant ChlF was excited with short measuring flashes (10–30 μs) and photochemistry was elicited by actinic light from the same set of orange Light Emitting Diodes (LED, 620 nm). The flashes were synchronized with the opening of the electronic shutter of the CCD camera (512×512 pixels, 12 bits) capturing the ChlF images. An optical filter RG695 was placed in front of the CCD camera that blocked the exciting light and allowed to measure the ChlF transient in the range 700–750 nm.

The quenching protocol with two sequentially applied levels of actinic light irradiance was used to measure the ChlF images. This protocol was already used earlier for discrimination between the healthy and infected tissue segments of *Arabidopsis thaliana* and is described in detail in [27, 28]. After measuring sequence of ChlF images, all the pixels of plants were separated from its background using a threshold subtraction. The threshold value was

chosen from the most contrasting image in the sequence. Using this technique, vectors of ChlF transients of all the plant pixels were extracted.

Data analysis tool

The ChlF images were analyzed using Matlab 6.5 and Pattern Recognition Toolbox PRTools v. 3.0 [32]. Algorithms of this toolbox randomly divide the data (vectors of ChlF transients in individual pixels) in two subsets: One subset of transients is used as a reference representing the species (classes) and the other subset is used to perform a simulated classification that serves to assess the algorithm performance. Eight classifiers and four feature selection algorithms were selected from the toolbox to study their efficiency for discrimination of the species.

Classifiers

Statistical classifier is a decision rule that assigns particular ChlF transient to one of the pre-defined classes. We tested the following eight classifiers for their performance and computation time requirement: Linear Discriminant Classifier (LDC) [33–35], Quadratic Discriminant Classifier (QDC) [36, 37], Fisher's Linear Discriminant Classifier (FLDC) [38], *k*-Nearest Neighbor Classifier (*k*-NNC) [39], Nearest Neighbor Classifier (NNC), Automatic Neural Network Classifier (NEURC) [36, 37], Support Vector Classifier (SVC) [40–43] and Nearest Mean Classifier (NMC) [44].

Evaluation of the classifier performance

The ChlF transients recorded in monoculture pots with basil (a), oregano (b), and sweet marjoram (c) plantlets were used for training and evaluating the classifiers performance. The transients were captured from three pots for each species in three consecutive days. Thus, each species was represented by several millions of transients captured in different pixels, representing different leaves and individual plants and taken at different times. Out of this enormous data set, we selected at random ca. 6,600 transients for each species. The thus selected sets of transients P_a, P_b, P_c representing transients of the plant species (a), (b), (c) were randomly and evenly divided into two pixel subsets each: (P_a^{train}, P_a^{test}), (P_b^{train}, P_b^{test}), and (P_c^{train}, P_c^{test}), respectively. The training sets P_a^{train}, P_b^{train}, P_c^{train} were used as a reference to represent the species (a), (b), (c) whereas the mixed testing set ($P_a^{test}+P_b^{test}+P_c^{test}$) was used to evaluate the performance of individual classifiers. Transients arbitrarily chosen from the testing set ($P_a^{test}+P_b^{test}+P_c^{test}$) were compared with each of the training sets (P_a^{train}, P_b^{train}, P_c^{train}) and classified as belonging to one of the three species (a), (b), (c) using the classifier algorithm. The classification was then validated to be either true or false by confronting the classification result with the origin of the particular transient in plant species (a), (b), or (c). The performance of each of the investigated classifiers was quantified by a number between 0–1: value '0' meaning random classification (1/3 of classifications into 3 equally represented classes correct, 2/3 incorrect) and value '1' meaning that the classifier was 100% successful.

Feature selection

The ChlF transients were captured in extensive series of fluorescence images, called features in our study. Feature selection algorithms are designed to reduce the number of features (fluorescence images) for an effective classification [45]. The reduction is based on an identification of an image sub-set that contains the most useful information for plant species identification. Here, we investigated four feature selection methods: Individual Feature Selection (IFS), Sequential Forward Selection (SFS) [46], Sequential Backward Selection (SBS) [46], and Sequential Forward Floating Selection (SFFS) [47].

Table 1 Performance of eight different classifiers (0—random, 1–100% correct) and computation time with 9,900 (9,900/3 for each species) testing and 9,900 (9,900/3 for each species) training transients

Classifier	Performance	Execution time (s)
Linear Discriminant Classifier (LDC)	0.74	14
Linear Discriminant Classifier (LDC)	0.74	14
Quadratic Discriminant Classifier (QDC)	0.82	15
Fisher's Linear Discriminant Classifier (FLDC)	0.75	62
Automatic Neural Networks Classifier (NEURC)	0.77	1,060
k-Nearest Neighbor Classifier (*k*-NN) (*k*=3)	0.76	13,007
Nearest Neighbor Classifier (NN)	0.74	13,793
Support Vector Classifier (SVC)	0.73	28,006
Nearest Mean Classifier (NMC)	0.15	5

For computation we used personal computer with Intel(R) Celeron(R) 2.60 GHz processor and 1.25 GB of RAM.

Results

Classifier performance and execution time

We used eight different algorithms in a simulated classification that was aimed at evaluating their performance and computational time. The results are summarized in Table 1.

With each of the classifiers, we used typically 3,300 testing ChlF transients[1] from each of the three pots with basil (a), oregano (b), and sweet marjoram plantlets (c). These individual testing transients were compared one by one with the training transients of the three species. By that, the algorithms classified each of the testing transients to one of the three species and the classification was counted either as false or correct depending on the true origin of the training transient. With known numbers of correct and false classifications for each of them, the performance of the classifiers was renormalized to 0 if completely random (1/3 of correct classifications in three equally represented classes) and to 1 for 100% of correct classifications. The performance results are shown in the second column of Table 1. Seven out of eight classifiers performed in a narrow range from 0.73 to 0.82.

Table 1 also shows in its third column the computational time required to classify the given number of testing transients. The nearest mean classifier was by far the fastest (5 s) classifier that, however, exhibited the poorest performance. On the other extreme, Quadratic Discriminant Classifier (15 s), and Linear Discriminant Classifier (14 s), and Fisher's Linear Discriminant Classifier (62 s) required low computation time and, yet, exhibited a high performance of species discrimination. Therefore, we choose to continue further evaluation only with Quadratic Discriminant Classifier (QDC) and with Linear Discriminant Classifier (LDC).[2]

Training set size

Another key property of the classifiers affecting their computation time requirement was the size of the training sets that was required for their optimal performance. Figure 1 shows the performance of the two most efficient classifiers, QDC and LDC, increasing with increasing size of the training sets. Above 500 training ChlF transients, the performance of LDC (solid line) started steeply increasing and reached to ca. 0.74 with ca. 3,500 training ChlF transients. A similar but less steep increase in performance

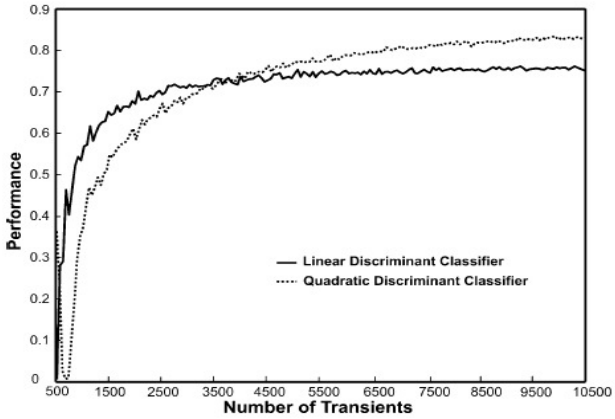

Fig. 1 The performance of the linear (*solid line*) and of the quadratic (*dotted line*) discriminant classifiers as they increase with the number of transients in the training set

was also observed with QDC (dotted line). The QDC classifier kept increasing to ca. 0.82 and outperformed LDC at the training set size larger than 4,500 transients (Fig. 1).

In the classifications documented in Fig. 1 and in Table 1, we used each of the 247 images capturing the entire ChlF transient in our experiments. However, one can possibly assume that some of the images show nearly identical information, such as repeatedly recorded images of F_M or F_0, whereas some other images within the fluorescence transient may be highly contrasting. The most contrasting images can be identified by feature selection algorithms that search for a small subset of features (images) that yield classification performance approaching or even exceeding the performance of the full image sequence. With such a reduced and optimized feature set, one can perform classification more effectively and faster than with the full image sequence.

Comparison of four feature selection methods using the best classifier QDC

Figure 2 shows the performance of QDC when the simulated classification is executed using a reduced number of fluorescence images. Earlier, Tyystjarvi et al. [22] choose to reduce the number of relevant features empirically. Here, we used and compared several feature selection algorithms in an effort to optimize the procedure (Fig. 2).

The reduced set of the ChlF images was identified by four different feature selection algorithms: Individual Feature Selection (IFS), Sequential Forward Selection (SFS), Sequential Backward Selection (SBS) and Sequential Forward Floating Selection (SFFS). The poorest performing algorithm was the Individual Feature Selection (IFS) that evaluated the performance of each single image and choose "the best individual performers" that, under-

[1] Somewhat smaller sets were used with the slower algorithms: with the automatic neural networks classifier (2,250 transients) and with the support vector classifier (1,350 transients) was used for both training and testing set for each species.

[2] The Fisher's Linear Discriminant Classifier is closely related to the Linear Discriminant Classifier.

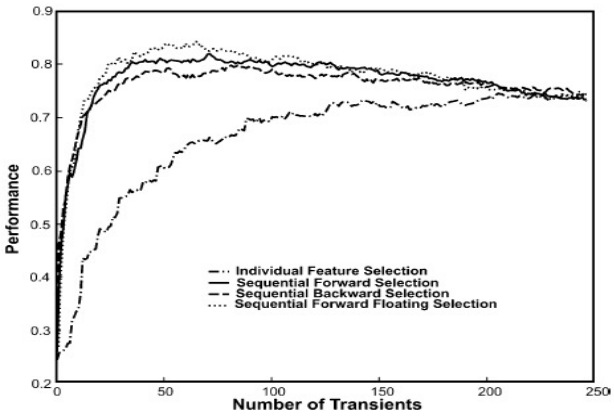

Fig. 2 Performance of the Quadratic Discriminant Classifier, QDC that was applied using a reduced number of fluorescence images that were identified by four algorithms: Individual Feature Selection, Sequentional Forward Selection, Sequentional Backward Selection and Sequentional Forward Floating Selection

standably failed in comparison with "the best performing feature teams". The failure can be understood when considering the model situation in which N images capture the same dynamic feature such as F_0. Assuming that this feature is yielding the highest contrast, these N images will all be selected by IFS in spite of the fact that they contain the same information and the classification performance does not increase with adding more images of the same type. The other feature selection algorithms choose also the best performer but then look for a teammate feature that leads to the highest performance enhancement. This is the principle of the Sequential Forward Selection (SFS). In an alternate way, the algorithm can also work backwards and eliminate from the whole feature set the data that, when not considered in the classification, do not reduce or reduce minimally the overall classification performance. This is the principle of the Sequential Backward Selection (SBS). Slightly better performance was found with training subsets of ChlF images identified by SFS compared to those identified by SBS. The best performing training sub-sets of fluorescence images were found with the SFFS. The highest performance was achieved with approximately a subset of ca. 50–100 images (Fig. 2)[3].

[3] One should note that the feature selection techniques investigated here do not analyze all potential combinations of fluorescence images and in this sense they are called suboptimal. We choose this approach to maintain feasibility with present high performance personal computers. Because of that unexpected time consumption it was impossible to apply optimal techniques such as branch and bound [48], however it would significantly increase the classification performance of the reduced feature sets.

Comparing images obtained with conventional ChlF parameters and with combinatorial imaging

Figure 3 presents the images of three conventional fluorescence parameters: F_0, F_M, and F_V/F_M for a pot in which a random mixture of the three species was grown. The F_0 (Fig. 3a) and F_M (Fig. 3b) signals are largely heterogeneous with slightly higher signals around the center of the image than at its periphery. This effect is probably due to the uncorrected instrument sensitivity profile used in our experiments. Also, the ChlF signals emitted from leaf margins tend to be lower than from the central leaf segments. No obvious dominant classification was observed for individual plants of either species. The F_V/F_M (Fig. 3c) signals are much more homogeneous than F_0 (Fig. 3a) and F_M (Fig. 3b) because the variability due to non-uniform illumination and sensitivity is reduced in ratio. Yet, no dominant species classification was found in Fig. 3c.

In contrast, Fig. 4 represents the classification of individual pixels by the Quadratic Discriminant Classifier, QDC that was used with a sub-set of 50 ChlF images that were identified by the Sequential Forward Floating Selection, SFFS algorithm. Clearly, the top row in Fig. 4 shows that the classification was successful when applied on single species pots.[4] The Fig. 4a shows a pot with basil (*Ocimum basilicum*, L.) that was mostly classified correctly (red color) with only few pixels classified erroneously by green color as oregano (*Origanum vulgare*, L.) and by blue color as majoram (*Origanum majorana*, L.). The pot in Fig. 4b with oregano was also mostly classified correctly (green color) with only few pixels classified erroneously by red color as sweet basil and few by blue color as marjoram. Similarly, the classification of marjoram in Fig. 4c was dominantly correct (blue color).

Figure 4d shows classification result in a more realistic situation where all the species were mixed in a single pot. In contrast to the conventional ChlF parameters shown in Fig. 3, the combinatorial imaging shown in Fig. 4d leads to a clear contrast with red pixels classified as basil (large leaves) contrasting with the two other two species: blue pixels classified as sweet marjoram, and green pixels as oregano.

Discussion

The simplest and most intuitive among the classifiers tested is the nearest mean classifier, NMC, which is representing each species by a single transient that is obtained by

[4] These pots were different from those used for classifier training.

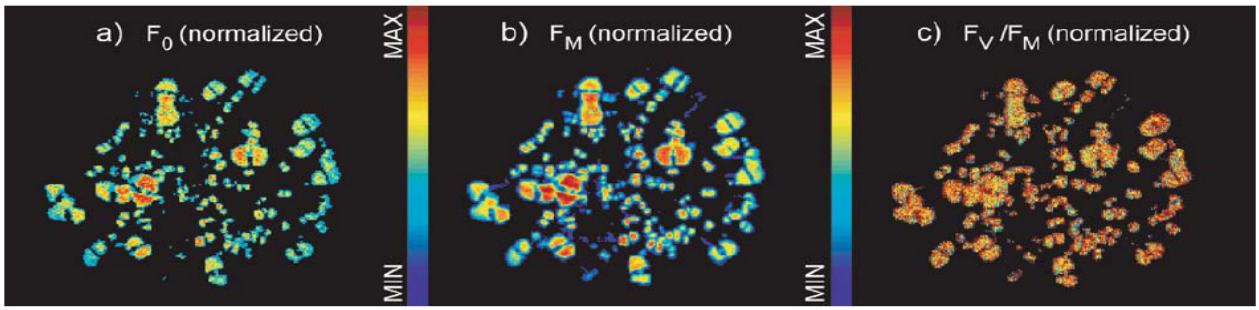

Fig. 3 The images **a**, **b**, and **c** represent the conventional fluorescence parameters F_0, F_M and F_V/F_M of a pot with randomly mixed specie. The fluorescence parameters are shown using a rainbow false color scale with minimum values shown in blue and maximum values shown in red. Normalization was done by subtracting the minimum value and further division by the difference between maximum minus minimum value, i.e. $\frac{F-\min(F)}{\max(F)-\min(F)}$

averaging all transients in the respective training class [44]. Unknown transients are then compared with each of the averaged representative transients of the individual species and classified to the species that is the most similar. The performance of this classifier was found in our experiments to be very low around 0.15 (Table 1). The NMC classifier failed because it does not reflect width of the statistical distribution in the training classes.

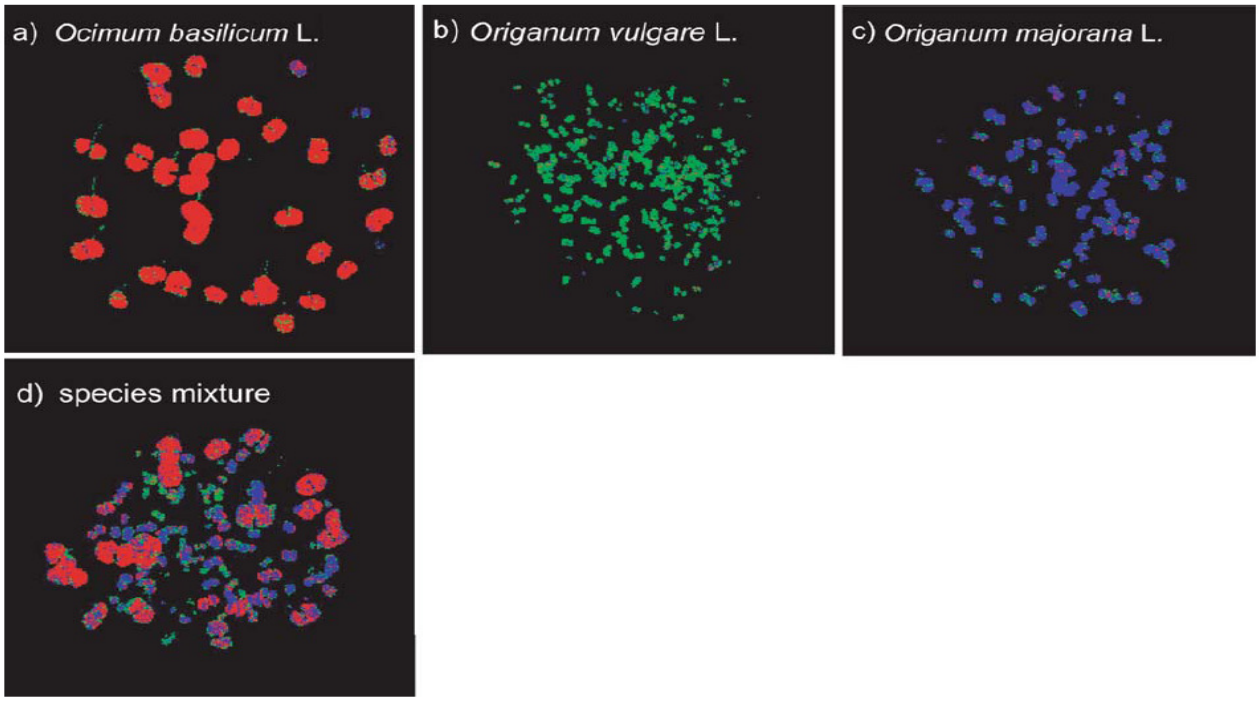

Fig. 4 The panels **a**, **b**, and **c** show QDC classification of fluorescence transients in individual pixels of images with pots containing seedlings of basil (*Ocimum basilicum*, L.), oregano (*Origanum vulgare*, L.) and marjoram (*Origanum majorana*, L.). The pixels classified as sweet basil are shown in *red*, those classified as oregano are shown in *green* and the pixels classified as marjoram are shown in *blue*. The same color code of classification is used in panel **d** that shows a pot in which all the three species grew mixed together

The other seven classifiers were of similarly high performance (0.73 to 0.82). Among these, we selected the best classifier based on its computation time. The computation time of the Support Vector Classifier (SVC) was the longest (ca. 8 h with a standard PC, Table 1). The long computation time of SVC was required for transformation of the original data into a space of a higher dimension that was followed by finding a linear separating surface between the two classes [49]. The *k*-Nearest Neighbor Classifier (*k*-NN), the Nearest Neighbor Classifier (NN) and the Automatic Neural Networks Classifier (NEURC) were also requiring excessive computation time. The optimal combination of high performance with acceptable computation time was found with the Quadratic Discriminant Classifier (QDC) (performance 0.82 in 15 s of computation time). The Linear Discriminant Classifier (LDC) achieved the second best classification performance of ca. 0.74 with 14 s of the computation time. The LDC and QDC identify a linear and quadratic hyperplane, respectively, that best separates the training transients of the individual species. The classification consists in finding on which side of the hyperplane the classified transient is. The classification performance of QDC (0.82) was better than that of the LDC (0.74) because the training classes were of different distribution leading to different covariance matrices and, eventually, to non-linear separating hyperplane.

With QDC and LDC identified as the two best performing classifiers, one needs to optimize the size of the training sets [50]. This was done by investigating the classification performance with increasing size of training data sets (Fig. 1). With very small training data sets the performance was not stable as the number of training transients was not sufficient to reliably place the classification hyperplane. The performance of LDC rapidly increased with increasing the number of training transients to 3,500. Above 3,500 training transients the position of the linear hyperplane was near to optimum and addition of training transients to 4,500 and more led to no improvement of performance. Optimal placing of a quadratic hyperplane that separates the transients of two species is harder and requires more training data. Thus, the performance of QDC was increasing less steeply compared to LDC and outperformed LDC only with ca. 4,500 training transients. In contrast to LDC, the QDC performance continued increasing above 8,100 training ChlF transients where we choose to limit our search because of computation time limits.

With QDC as the best classifier, we further optimized the species discrimination by feature selection. Both SFS and SBS are more effective than IFS (Fig. 2). The best results were obtained with the Sequential Forward Floating Selection (SFFS). The SFFS works in the similar way as SFS algorithm, but after every addition of an image, it checks if removing another image from the selection would not lead to a better performance than one step back. By checking such potential "backward steps", the SFFS algorithm identified feature sets that were performing slightly better than the sets found by SFS or SBS (Fig. 2). In our experiments, the SFFS algorithm reduced the full data set of 247 images to 50 images that were the most effective. The classification with 50 images was significantly faster than with the full data set (247 images) without compromising the classification performance.

Our results show that the Quadratic Discriminant Classifier (QDC) utilizing only 50 images found by the Sequential Forward Floating Selection (SFFS) constitutes a robust and effective method for plant species discrimination based on ChlF transients. In our simulated species discrimination, the conventional ChlF parameters such as F_0, F_M, and F_V/F_M shown in Fig. 3 as well as other conventional parameters that were tested but not shown (NPQ, qP, Rfd) failed. The low discriminative potential of these parameters is understandable because the closely related plants have similar chlorophyll density in leaves, similar leaf structure and similar photosynthetic yield [40, 51]. The natural variability of the ChlF emission and low contrast between the closely related species do not allow effective species discrimination.

In contrast, the combinatorial species discrimination represented in Fig. 4 was highly effective. When tested with a pot in which all three species were mixed (Fig. 4d) the contrast between the species was preserved although some erroneously classified pixels were detected, probably, because of leaf overlaps that were prominent in the two small leaf species (oregano and marjoram). The classification of basil with large leaves was typically correct even in the pot with mixed species (basil).

Acknowledgement The work was supported by the Czech Ministry of Education, Sports and Youth under the Grant MSM6007665808, by the Czech Academy of Sciences Grant AV0Z60870520.

References

1. Feyaerts F, van Gool L (2001) Multi-spectral vision system for weed detection. Pattern Recognit Lett 22(6–7):667–674. doi:10.1016/S0167-8655(01)00006-X
2. Kavdir I (2004) Discrimination of sunflower, weed and soil by artificial neural networks. Comput Electron Agric 44(2):153–160. doi:10.1016/j.compag.2004.03.006
3. Gerhards R, Christensen S (2003) Real-time weed detection, decision making and patch spraying in maize, sugar beet, winter wheat and winter barley. Weed Res 43(6):385–392. doi:10.1046/j.1365-3180.2003.00349.x
4. Timmermann C, Gerhards R, Kuhbauch W (2003) The economic impact of site-specific weed control. Precis Agric 4(3):249–260. doi:10.1023/A:1024988022674

5. Wang N, Zhang N, Dowell FE, Sun Y, Peterson DE (2001) Design of an optical weed sensor using plant spectral characteristics. Trans ASAE 44(2):409–419
6. El-Faki MS, Zhang N, Peterson DE (2000) Weed detection using color machine vision. Trans ASAE 43(6):1969–1978
7. Cho SI, Lee DS, Jeong JY (2002) Weed-plant discrimination by machine vision and artificial neural network. Biosystems Eng 83 (3):275–280. doi:10.1006/bioe.2002.0117
8. Franz E, Gebhardt MR, Unklesbay KB (1995) Algorithms for extracting leaf boundary information from digital images of plant foliage. Trans ASAE 38(2):625–633
9. Gerhards R, Kuhbauch W (1993) Dynamic decision-model for weed control methods in cereals by means of digital image analysis. J Agron Crop Sci 171(5):329–335. doi:10.1111/j.1439-037X.1993.tb00148.x
10. Tian LF, Slaughter DC (1998) Environmentally adaptive segmentation algorithm for outdoor image segmentation. Comput Electron Agric 21(3):153–168. doi:10.1016/S0168-1699(98)00037-4
11. Lee WS, Slaughter DC, Giles DK (1999) Robotic weed control system for tomatoes. Precis Agric 1:95–113
12. Haggar RJ, Stent CJ, Isaac S (1983) A prototype hand-held patch sprayer for killing weeds, activated by spectral differences in crop weed canopies. J Agric Eng Res 28(4):349–358. doi:10.1016/0021-8634(83)90066-5
13. Felton WL, McCloy KR (1992) Spot spraying. Agric Eng 73 (6):9–12
14. Shiraishi M, Sumiya H (1996) Plant identification from leaves using quasi-sensor fusion. J Manuf Sci Eng Trans ASME 118 (3):382–387. doi:10.1115/1.2831041
15. Vrindts E, De Baerdemaeker J (2000) Using spectral information for weed detection in field circumstances. AgEng 2000 Conference, Warwick, UK
16. Scotford IM, Miller PCH (2005) Applications of spectral reflectance techniques in northern European cereal production: a review. Biosystems Eng 90(3):235–250
17. Govindjee (1995) 63 years since Kautsky—Chlorophyll a fluorescence. Aust J Plant Physiol 22(2):131–160
18. Nedbal L, Whitmarsh J (2004) Chlorophyll fluorescence imaging of leaves and fruits. In: Papageorgiu G, Govindjee (eds) Chlorophyll a fluorescence: A signature of photosynthesis. Springer, Dordrecht, The Netherland, pp 389–407
19. Balachandran S, Osmond CB, Daley PF (1994) Diagnosis of the earliest strain-specific interactions between tobacco-mosaic-virus and chloroplasts of tobacco leaves in-vivo by means of chlorophyll fluorescence imaging. Plant Physiol 104(3):1059–1065
20. Chaerle L, Hagenbeek D, De Bruyne E, Valcke R, Van der Straeten D (2004) Thermal and chlorophyll-fluorescence imaging distinguish plant-pathogen interactions at an early stage. Plant Cell Physiol 45(7):887–896. doi:10.1093/pcp/pch097
21. Lazar D, Susila P, Naus J (2006) Early detection of plant stress from changes in distributions of chlorophyll a fluorescence parameters measured with fluorescence imaging. J Fluoresc 16 (2):173–176. doi:10.1007/s10895-005-0032-1
22. Tyystjärvi E, Koski A, Keranen M, Nevalainen O (1999) The Kautsky curve is a built-in barcode. Biophys J 77(2):1159–1167
23. Keranen M, Aro EM, Tyystjarvi E, Nevalainen O (2003) Automatic plant identification with chlorophyll fluorescence fingerprinting. Precis Agric 4(1):53–67. doi:10.1023/A:1021863005378
24. Bennedsen BS, Rasmussen P, Nielsen H (2000) Crop growth information from line spectrometer data using neural networks. AgEng 2000 Conference, Warwick, UK
25. Jayas DS, Paliwal J, Visen NS (2000) Multi-layer neural networks for image analysis of agricultural products. J Agric Eng Res 77 (2):119–128. doi:10.1006/jaer.2000.0559
26. Lichtenthaler HK, Buschmann C, Knapp M (2005) How to correctly determine the different chlorophyll fluorescence parameters and the chlorophyll fluorescence decrease ratio R_{Fd} of leaves with the PAM fluorometer. Photosynthetica 43(3):379–393. doi:10.1007/s11099-005-0062-6
27. Matous K, Benediktyova Z, Berger S, Roitsch T, Nedbal L (2006) Case study of combinatorial imaging: what protocol and what chlorophyll fluorescence image to use when visualizing infection of *Arabidopsis thaliana* by *Pseudomonas syringae?*. Photosynth Res 90(3):243–253. doi:10.1007/s11120-006-9120-6
28. Berger S, Benediktyova Z, Matous K, Bonfig K, Mueller MJ, Nedbal L, Roitsch T (2007) Visualization of dynamics of plant-pathogen interaction by novel combination of chlorophyll fluorescence imaging and statistical analysis: differential effects of virulent and avirulent strains of *P. syringae* and of oxylipins on *A. thaliana*. J Exp Bot 58(4):797–806. doi:10.1093/jxb/erl208
29. Codrea CM, Aittokallio T, Keranen M, Tyystjarvi E, Nevalainen OS (2003) Feature learning with a genetic algorithm for fluorescence fingerprinting of plant species. Pattern Recognit Lett 24(15):2663–2673. doi:10.1016/S0167-8655(03)00109-0
30. Siedlecki W, Sklansky J (1989) A note on genetic algorithms for large-scale feature selection. Pattern Recognit Lett 10(5):335–347. doi:10.1016/0167-8655(89)90037-8
31. Nedbal L, Soukupova J, Kaftan D, Whitmarsh J, Trtilek M (2000) Kinetic imaging of chlorophyll fluorescence using modulated light. Photosynth Res 66(1–2):3–12. doi:10.1023/A:1010729821876
32. Duin RPW (2000) PRTools- version 3.0- A Matlab toolbox for pattern recognition
33. Fukunaga K (1990) Introduction to statistical pattern recognition, 2nd edn. Academic Press Professional, San Diego, USA
34. Martinez AM, Kak AC (2001) PCA versus LDA. IEEE Trans Pattern Anal Mach Intell 23(2):228–233. doi:10.1109/34.908974
35. Wang XC, Paliwal KK (2003) Feature extraction and dimensionality reduction algorithms and their applications in vowel recognition. Pattern Recognit 36(10):2429–2439. doi:10.1016/S0031-3203(03) 00044-X
36. Bishop CM (1995) Neural networks for pattern recognition. Oxford University Press
37. Jain AK, Mao JC, Mohiuddin KM (1996) Artificial neural networks: a tutorial. Computer 29(3):31–44. doi:10.1109/2.485891
38. Fisher R (1936) The use of multiple measurements in taxonomic problems. Ann Eugen 7:179–188
39. Fukunaga K, Hostetler LD (1975) K-nearest-neighbor Bayes-risk estimation. IEEE Trans Inf Theory 21(3):285–293. doi:10.1109/TIT.1975.1055373
40. Munne-Bosch S, Nogues S, Alegre L (1999) Diurnal variations of photosynthesis and dew absorption by leaves in two evergreen shrubs growing in Mediterranean field conditions. New Phytol 144(1):109–119. doi:10.1046/j.1469-8137.1999.00490.x
41. Boser B, Guyon I, Vapnik V (1992) A training algorithm for optimal margin classifiers. COLT 92: Proceedings of the 5th annual workshop on computational learning theory. ACM
42. Brown M, Gunn SR, Lewis HG (1999) Support vector machines for optimal classification and spectral unmixing. Ecol Modell 120 (2–3):167–179. doi:10.1016/S0304-3800(99)00100-3
43. Camps-Valls G, Gomez-Chova L, Calpe-Maravilla J, Martin-Guerrero JD, Soria-Olivas E, Alonso-Chorda L, Moreno J (2004) Robust support vector method for hyperspectral data classification and knowledge discovery. IEEE Trans Geosci Rem Sens 42 (7):1530–1542. doi:10.1109/TGRS.2004.827262
44. McQueen J (1967) Some methods for classification and analysis of multivariate observations, In Proc. of the 5th Berkeley symposium on mathematical statistics and probability
45. Jain AK, Duin RPW, Mao JC (2000) Statistical pattern recognition: a review. IEEE Trans Pattern Anal Mach Intell 22(1):4–37. doi:10.1109/34.824819

46. Kittler J (1978) Feature set search algorithms. Pattern Recognit Signal Process 41–60
47. Pudil P, Novovicova J, Kittler J (1994) Floating search methods in feature selection. Pattern Recognit Lett 15(11):1119–1125. doi:10.1016/0167-8655(94)90127-9
48. Somol P, Pudil P, Kittler J (2004) Fast branch & bound algorithms for optimal feature selection. IEEE Trans Pattern Anal Mach Intell 26(7):900–912. doi:10.1109/TPAMI.2004.28
49. Lau KW, Wu QH (2003) Online training of support vector classifier. Pattern Recognit 36(8):1913–1920. doi:10.1016/S0031-3203(03) 00038-4
50. Chtioui Y, Bertrand D, Barba D (1996) Reduction of the size of the learning data in a probabilistic neural network by hierarchical clustering. Application to the discrimination of seeds by artificial vision. Chemom Intell Lab Syst 35(2):175–186. doi:10.1016/S0169-7439(96)00065-2
51. Whitehead D, Walcroft AS, Scott NA, Townsend JA, Trotter CM, Rogers GND (2004) Characteristics of photosynthesis and stomatal conductance in the shrub land species manuka (*Leptospermum scoparium*) and kanuka (*Kunzea ericoides*) for the estimation of annual canopy carbon uptake. Tree Physiol 24 (7):795–804

4.2 Chlorophyll fluorescence emission as a reporter on freezing tolerance in *Arabidopsis thaliana* accessions

Plant signaling & Behavior, 2011

Anamika Mishra, Kumud B. Mishra, Imke I. Höermiller, Arnd G. Heyer, Ladislav Nedbal

Abstract

Non-invasive, high-throughput screening methods are valuable tools in breeding for abiotic stress tolerance in plants. Optical signals such as chlorophyll fluorescence emission can be instrumental in developing new screening techniques. In order to examine the potential of chlorophyll fluorescence to reveal plant tolerance to low temperatures, we used a collection of nine *Arabidopsis thaliana* accessions and compared their fluorescence features with cold tolerance quantified by the well established electrolyte leakage method on detached leaves. We found that, during progressive cooling, the minimal chlorophyll fluorescence emission rose strongly and that this rise was highly dependent on the cold tolerance of the accessions. Maximum quantum yield of PSII photochemistry and steady state fluorescence normalized to minimal fluorescence were also highly correlated to the cold tolerance measured by the electrolyte leakage method. In order to further increase the capacity of the fluorescence detection to reveal the low temperature tolerance, we applied combinatorial imaging that employs plant classification based on multiple fluorescence features. We found that this method, by including the resolving power of several fluorescence features, can be well employed to detect cold tolerance already at mild sub-zero temperatures. Therefore, there is

no need to freeze the screened plants to the largely damaging temperatures of around -15°C. This, together with the method's easy applicability, represents a major advantage of the fluorescence technique over the conventional electrolyte leakage method.

RESEARCH PAPER

Plant Signaling & Behavior 6:2, 1-10; February 2011; ©2011 Landes Bioscience

Chlorophyll fluorescence emission as a reporter on cold tolerance in *Arabidopsis thaliana* accessions

Anamika Mishra,[1,2] Kumud B. Mishra,[2,*] Imke I. Höermiller,[3] Arnd G. Heyer[3] and Ladislav Nedbal[2]

[1]Institute of Physical Biology, University of South Bohemia, Nové Hrady, Czech Republic; [2]CzechGlobe - Global Change Research Centre, Academy of Science of Czech Republic, Nové Hrady, Czech Republic; [3]Biologisches Institut, Abt. Botanik, Universität Stuttgart, Stuttgart, Germany

Key words: chlorophyll fluorescence, cold acclimation, electrolyte leakage, high-throughput screening, natural accessions

Abbreviations: F_0, minimal fluorescence emission of a dark adapted plant with primary acceptor; Q_A, oxidized and non-photochemical quenching inactive; F_m, maximum fluorescence emission of a dark adapted plant exposed to a short pulse of a strong light leading to a transient reduction of Q_A; F_v, variable fluorescence ($F_v=F_m-F_0$); F_v/F_m, ratio interpreted as the maximum quantum yield of PSII photochemistry; P, fluorescence peak at the beginning of the transient with actinic light; M, the secondary maxima of the chlorophyll fluorescence transients subsequent to peak P; F_s,steady state fluorescence; PSII, Photosystem II; PSI, Photosystem I; EL, electrolyte leakage; LT_{50EL}, the temperature (lethal temperature) at which 50% of electrolyte leakage occurs when measured by conductivity in a freeze-thaw cycle

Non-invasive, high-throughput screening methods are valuable tools in breeding for abiotic stress tolerance in plants. Optical signals such as chlorophyll fluorescence emission can be instrumental in developing new screening techniques. In order to examine the potential of chlorophyll fluorescence to reveal plant tolerance to low temperatures, we used a collection of nine *Arabidopsis thaliana* accessions and compared their fluorescence features with cold tolerance quantified by the well established electrolyte leakage method on detached leaves. We found that, during progressive cooling, the minimal chlorophyll fluorescence emission rose strongly and that this rise was highly dependent on the cold tolerance of the accessions. Maximum quantum yield of PSII photochemistry and steady state fluorescence normalized to minimal fluorescence were also highly correlated to the cold tolerance measured by the electrolyte leakage method. In order to further increase the capacity of the fluorescence detection to reveal the low temperature tolerance, we applied combinatorial imaging that employs plant classification based on multiple fluorescence features. We found that this method, by including the resolving power of several fluorescence features, can be well employed to detect cold tolerance already at mild sub-zero temperatures. Therefore, there is no need to freeze the screened plants to the largely damaging temperatures of around -15°C. This, together with the method's easy applicability, represents a major advantage of the fluorescence technique over the conventional electrolyte leakage method.

Introduction

Susceptibility to low temperature limits the geographical distribution of plants in temperate and polar zones and can also adversely influence crop yields. Counteracting the limitation, many plant species are able to increase their low temperature tolerance by an acclimation to suboptimal temperatures.[1] The cold acclimation includes complex cellular and biochemical changes such as altered membrane composition, accumulation of soluble sugars, proline, as well as the production of antifreeze proteins.[2-5] In winter cereals6 and in *Arabidopsis thaliana*,[7-8] the cold acclimation was shown to result in an increased photosynthetic activity. The capacity to acclimate to low temperature largely deviates in accessions of *Arabidopsis thaliana* originating from warm and cool climate habitats. The contrast in acclimation capacity in *A. thaliana* accessions has already been extensively exploited in efforts to identify the molecular basis of this trait.[9-11] The resulting enhanced capacity of acclimated plants to survive subzero temperatures may be due to freezing tolerance and/or avoidance mechanisms. While freezing tolerant plants do not prevent formation of ice crystals in the extracellular space but, rather, limit the damage to cellular structures by the ice crystals, it has been reported that Arabidopsis survives low temperatures by freezing avoidance, i.e. by preventing ice crystal formation via supercooling of cellular and extracellular fluids.[12-13]

The research of cold tolerance/susceptibility largely relies on methods that can precisely measure the temperature at which irreversible damage occurs to the plants. The classical methods

*Correspondence to: Kumud Bandhu Mishra; mishra@greentech.cz
Submitted: 01/07/11; Revised: 02/24/11; Accepted: 02/24/11
DOI: 10.4161/psb/6.2.15278

a freeze-thaw cycle. Therefore, we determined the LT_{50EL} of *A. thaliana* accessions (**Fig. 1**) as a reference to evaluate the potential of fluorescence analysis. The most tolerant accession Te exhibits the lowest LT_{50EL} value of –12.2 °C followed by Rsch (LT_{50EL} = -10.6 °C), and Col-0 (LT_{50EL} = -10.3 °C). Intermediate cold tolerance was found in Ler (LT_{50EL} = -8.7 °C) and in Nd (LT_{50EL} = -7.8 °C). The sensitive accessions: Co, Can, Cvi, and C24 that originate from warm climate zones have a LT_{50EL} of approximately -6 °C. Calculation of the 95% confidence intervals revealed three significantly deviating groups consisting of the four sensitive accessions, the intermediate accessions Ler and Nd and the tolerant accessions Col-0, Rsch and Te, respectively.

Chlorophyll fluorescence emission

Chlorophyll fluorescence parameters. The measurement of chlorophyll fluorescence emission during cooling of the leaves from 4 °C down to -15 °C revealed dramatic modulation of basic fluorescence parameters (**Fig. 2**). The minimum fluorescence, F_0, remained largely insensitive to cooling of the leaves until ca. -6 °C. A further decrease of the leaf temperature led to a significant increase of F_0. A sharp non-linear increase of F_0 below ca. -6 °C was observed in *A. thaliana* accessions that were identified as cold sensitive by the electrolyte leakage experiments. These accessions, Co, Can, Cvi, and C24, are represented in Figure 2A by blue lines. The increase of F_0 towards lower temperatures was much weaker in the accessions Ler and Nd (**green lines in Fig. 2A**) that were identified as moderately tolerant. The tolerant accessions Te, Rsch and Col-0 displayed only a small variation of F_0 at low temperatures (**red lines in the Fig. 2A**).

Figure 2B shows the temperature dependence of the maximum fluorescence yield, F_m, for all nine *A. thaliana* accessions. F_m remained approximately constant at temperatures above -4 °C with the exception of C24, where a decrease occurred at temperature below -1 °C (**Fig. 2B**). Below -4 °C, Fm was decreasing with lowering of the temperature. In contrast to F_0, the trends in the F_m temperature dependence in the nine *A. thaliana* accessions were variable to an extent that prevented a clear distinction of low temperature tolerance classes.

Figure 2C shows that the steady state fluorescence emission F_s attained in actinic irradiance [40 µmol (photons) $m^{-2}s^{-1}$] was negatively correlated with temperature below 0 °C. The onset of the F_s modulation (**Fig. 2C**) occurred at a higher temperature as compared to F_0 (**Fig. 2A**). However, the difference between the sensitive and tolerant accessions is not apparent in F_s to the extent observed for F0. Under high actinic light [120 µmol (photons) $m^{-2}s^{-1}$] the changes of F_s among different accessions were less prominent (data not shown).

The fluorescence parameters shown in **Figure 2** are absolute signal levels digitized for each camera pixel and

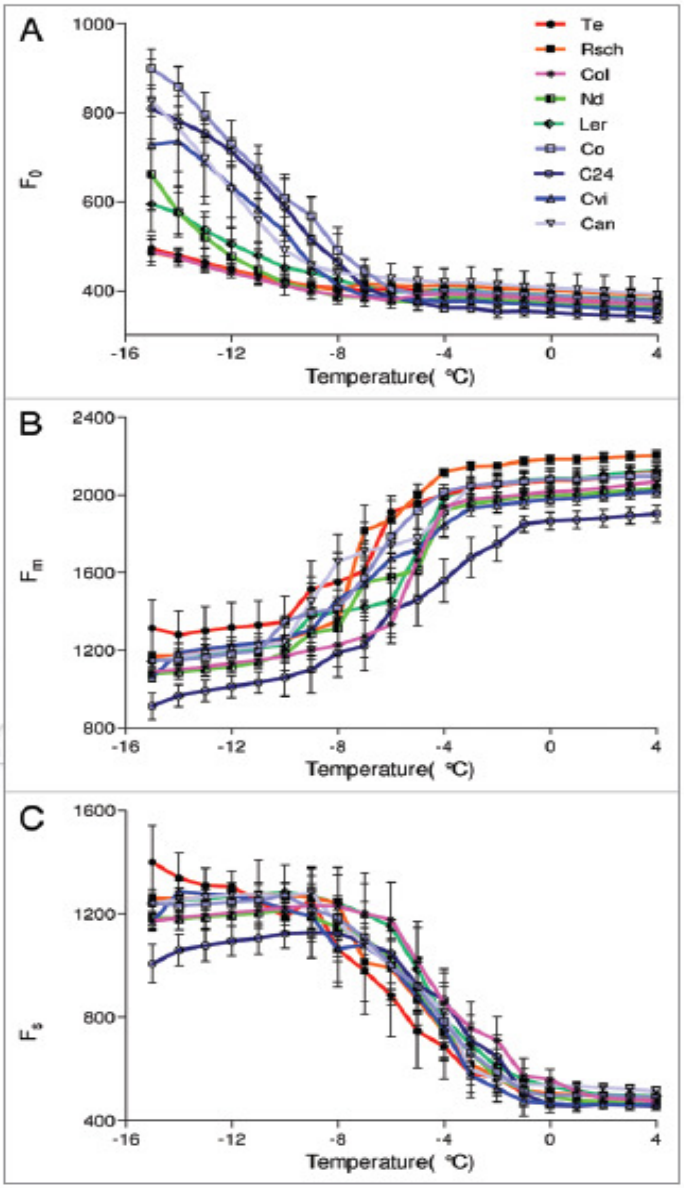

Figure 2. Chlorophyll fluorescence emission yields as a function of leaf temperature from 4 °C down to -15 °C for nine investigated accessions of *A. thaliana*. (A) minimal fluorescence, F_0, (B) maximal fluorescence, F_m, and (C) steady state fluorescence, F_s. The graphs show means and standard deviations obtained in five independent experiments.

4.3 Engineered drought tolerance in tomato plants is reflected in chlorophyll fluorescence emission.

Plant Science, 2011

Kumud B. Mishra, R. Iannacone, Angelo Petrozza, Anamika Mishra, Nadia Armentano, Giovanna La Vecchia, Martin Trtílek, Francesco Cellini, Ladislav Nedbal

Abstract

Drought stress is one of the most important factors that limit crop productivity worldwide. In order to obtain tomato plants with enhanced drought tolerance, we inserted the transcription factor gene *ATHB-7* into the tomato genome. This gene was demonstrated earlier to confer drought tolerance in *Arabidopsis thaliana* by acting as a negative regulator of growth. We compared the performance of wild type and transgenic tomato line DTL-20, carrying *ATHB*-7 gene, under well irrigated and water limited conditions. We found that transgenic plants had reduced stomatal density and stomatal pore size and exhibited an enhanced resistance to soil water deficit. We used the transgenic plants to investigate the potential of chlorophyll fluorescence to report drought tolerance in a simulated high-throughput screening procedure. Wild type and transgenic tomato plants were exposed to drought stress lasting 18 days. The stress was then terminated by rehydration after which recovery was studied for another 2 days. Plant growth, leaf water potential, and chlorophyll fluorescence were measured during the entire experimental period. We found that water potential in wild type and drought tolerant transgenic plants diverged around 11^{th} day of stress. The chlorophyll fluorescence parameters: the non-photochemical quenching, effective quantum efficiency of PSII, and the

maximum quantum yield of PSII photochemistry yielded a good contrast between wild type and transgenic plants from 7^{th}, 12^{th}, and 14^{th} day of stress, respectively. We propose that chlorophyll fluorescence emission reports well on the level of water stress and, thus, can be used to identify elevated drought tolerance in high-throughput screens for selection of resistant genotypes.

5. Conclusions

In this thesis, chlorophyll *a* fluorescence signal was evaluated for discriminating between plant species and screening of cold and drought stress tolerance in plants. For this purpose, chlorophyll *a* fluorescence imaging was used with complex light/dark protocols (Nedbal et al., 2000a). Combinatorial imaging based on advanced statistical analysis of fluorescence image sequences for information extraction from large data sets has already been demonstrated to be superior over conventional chlorophyll fluorescence parameter analysis in visualizing virus infection at very early stages (Matouš et al., 2006). We have explored its application for discrimination between plant species of the same family (Mishra et al., 2009) and to identify cold tolerance in *Arabidopsis thaliana* accessions at non-lethal temperatures (Mishra et al., 2011), where conventional chlorophyll fluorescence parameters had failed. Furthermore, we have demonstrated in this thesis the physiological significance of conventional parameters Fv/Fm (variable to maximum fluorescence ratio), Φ_{PSII} (effective quantum yield of PS II) and NPQ (non-photochemical quenching of the excited state of Chl *a*) in several systems, and for sensing drought tolerance in tomato transgenic plants.

We believe that chlorophyll fluorescence based screening methods may be efficiently applied and developed for discriminating between weeds and crops at very early stage of their growth. This would be very useful for the automatic monitoring of fertilizers and insecticides in crop field. We suggest that chlorophyll based screening methods are very useful for the selection of stress tolerance genotypes and large scale screening of abiotic stress tolerance e.g. in recombinant inbred line populations or other plant sets consisting of individual plants representing different genotypes. The method is thus well suited for quantitative trait loci (QTL) mapping (Collard et al 2005) or mutant screening (Codrea et al, 2010) to identify genetic determinants of stress tolerance, which may be used for plant breeding.

6. Bibliography

Agati G, Cerovic ZG, Moya I (2000) "The effect of decreasing temperature up to chilling values on the in vivo F685/F735 chlorophyll fluorescence ratio in Phaseolus vulgaris and Pisum sativum: The role of the photosystem I contribution to the 735 nm fluorescence band." Photochem Photobiol 72 (1): 75-84

Arnon DI, Allen MB, Whatley FR (1954) "Photosynthesis by isolated chloroplasts." Nature 174: 394–396

Artus NN, Uemura M, Steponkus PL, Gilmour SJ, Lin CT, Thomashow MF (1996) "Constitutive expression of the cold-regulated Arabidopsis thaliana COR15a gene affects both chloroplast and protoplast freezing tolerance." Proc Natl Acad Sci USA 1996; 93(23): 13404-13409

Auirrezabal S, Bouchier-Combaud S, Radziejwoski A, Dauzat M, Cookson SJ, Granier C (2006) " Plasticity to soil water deficit in Arabidopsis thaliana: dissection of leaf development into underlying growth dynamic and cellular variables reveals invisible phenotypes." Plant Cell Environ 29: 2216–2227.

Baker NR, Rosenqvist E (2004) "Applications of chlorophyll fluorescence can improve crop production strategies: an examination of future possibilities." J Exp Bot 55(403): 1607-1621

Baker NR (2008) "Chlorophyll fluorescence: a probe of photosynthesis in vivo." Annual Review of Plant Biology 59: 89-113

Balachandran S, Osmond CB, Daley PF (1994) "Diagnosis of the earliest strain-specific interactions between tobacco-mosaic-virus and chloroplasts of tobacco leaves in-Vivo by means of chlorophyll fluorescence imaging." Plant Physiol 104(3):1059-1065

Bartels D, Scheneider K, Terstappen G, Piatkowski D, Salamini F (1990) "Molecular cloning of abscisic acid-modulation genes which are induced during desiccation of the resurrection plant Craterostigma plantagineum." Planta 181: 27– 34

Barth C, Krause GH (1999) "Inhibition of photosystems I and II in chilling-sensitive and chilling-tolerant plants under light and low-temperature stress." Zeitschrift für Naturforschung C, J Biosci 54(9-10): 645–657

Bennedsen BS, Rasmussen P, Nielsen H (2000) "Crop growth information from line spectrometer data using neural networks." AgEng 2000 Conference. Warwick, UK

Berger S, Benediktyova Z, Matous K, Bonfig K, Mueller MJ, Nedbal L, Roitsch T (2007) "Visualization of dynamics of plant-pathogen interaction by novel combination of chlorophyll fluorescence imaging and statistical analysis: differential effects of virulent and avirulent strains of P. syringae and of oxylipins on A. thaliana." J Exp Bot 58(4):797-806

Bhattacharyya A (1943) "On a measure of divergence between two statistical populations defined by their probability distributions." Bull Cal Math Soc 35: 99–110

Bhattacharyya A (1946) "On a measure of divergence between two multinomial populations." Sankhya 7: 401–406

Bishop CM (1995)" Neural networks for pattern recognition." Oxford University Press,

Blankenship RE (2002) Molecular mechanisms of photosynthesis. Blackwell Science Ltd, London, UK

Bodner M, Beck E (1987) "Effect of supercooling and freezing on photosynthesis in freezing tolerant leaves of Afroalpine gaint rosette plants." Oecologia 72: 366-371

Boser B, Guyon I, Vapnik V (1992) "A training algorithm for optimal margin classifiers. COLT 92: proceedings of the fifth annual workshop on computational learning theory." ACM

Boyer JS (2010) "Drought decision-making." J Exp Bot 61:3493-3497

Bradbeer JW (1977) "Chloroplasts- Structure and development. The molecular biology of plant cell." Blackwell scientific publications, California. 64-74

Bray EA (1993) "Molecular responses to water – deficit." Plant Physiol 103: 1035-1040

Bray EA, Bailey-Serres J, Weretilnyk E (2000) "Responses to abiotic stresses." In: Gruissem W, Buchannan BB, Jones RL (Eds), Biochemistry and Molecular Biology of Plants, American Society of Plant Physiologists, 1158-1249

Brown M, Gunn SR, Lewis HG (1999) "Support vector machines for optimal classification and spectral unmixing." Ecol Model 120(2-3):167-179

Buschmann C., Langsdorf G., Lichtenthaler H.K. (2000) Imaging of the blue, green and red fluorescence emission of plants: An overview. Photosynthetica 38: 483-491

Camps-Valls G, Gomez-Chova L, Calpe-Maravilla J, Martin-Guerrero JD, Soria-Olivas E, Alonso-Chorda L, Moreno J (2004) "Robust support vector method for hyperspectral data classification and knowledge discovery." IEEE Trans Geosci Remote Sensing 42(7):1530-1542

Castonguay Y, Markhart AH (1991) "Saturated rates of photosynthesis in water-stressed leaves of common bean and tepary bean." Crop Sci 31: 1605–1611

Catala R, Ouyang J, Abreu IA, Hu Y, Seo H, Zhang X, Chua NH (2007) "The arabidopsis E3 SUMO ligase SIZ1 regulates plant growth and drought responses." Plant Cell, 19: 2952–2966

Chaerle L, Hagenbeek D, De Bruyne E, Valcke R, Van der Straeten D (2004) "Thermal and chlorophyll-fluorescence imaging distinguish plant-pathogen interactions at an early stage." Plant Cell Physiol 45(7):887-896

Chaves MM, Maroco JP, Pereira JS (2003) "Understanding plant responses to drought — from genes to the whole plant." Funct Plant Biol 30: 239-264.

Chen Z, Newman I, Zhou M, Mendham N, Zhang G, Shabala S (2005) "Screening plants for salt tolerance by measuring K+ flux: a case study for barley." Plant Cell Environ 28:1230–1246.

Cho SI, Lee DS, Jeong JY (2002) "Weed-plant discrimination by machine vision and artificial neural network." Biosyst Eng 83(3):275-280

Chtioui Y, Bertrand D, Barba D (1996) "Reduction of the size of the learning data in a probabilistic neural network by hierarchical clustering. Application to the discrimination of seeds by artificial vision." Chemometrics Intell Lab Syst 35(2):175-186

Codrea CM, Aittokallio T, Keranen M, Tyystjarvi E, Nevalainen OS (2003) "Feature learning with a genetic algorithm for fluorescence fingerprinting of plant species." Pattern Recognit Lett 24(15):2663-2673

Codrea MC, Hakala-Yatkin M, Karlund-Marttila A, Nedbal L, Aittokallio T, Nevalainen OS, Tyystjävi E (2010) "Mahalanobis distance screening of Arabidopsis mutants with chlorophyll fluorescence." Photosynth Res 105: 273–283

Collard BCY, Jahufer MZZ, Brouwer JB, Pang ECK (2005) "An introduction to markers, quantitative trait loci (QTL) mapping and marker-assisted selection for crop improvement: The basic concepts." Euphytica 142(1-2): 169-196

Daugherty CJ, Rooney MF, Paul AL, deVetten N, Vega-Palas M, Lu G, Gurley WB, Ferl RJ (1994) "Environmental stress and gene regulation." In: Meyerowitz EM, Somerville CR (Eds) Arabidopsis, Cold Spring. Harbor Laboratory Press, Cold Spring Harbor, NY, USA, 769–806

Dau H (1994) "Molecular mechanisms and quantitative models of variable Photosystem II fluorescence." Photochem Photobiol 60:1–23

Demeter S, Rozsa Z, Vass I, Hideg E (1985) "Thermo-luminescence study of charge recombination in photosystem-II at low temperatures.2. Oscillatory properties of the ZV and thermo-luminescence bands in chloroplast dark-adapted for various time periods." Biochim Biophys Acta 809(3): 379–387

Demming-Adams B, Gilmore AM, Adams WW (1996) "In vivo functions of carotenoids in higher plants." FASEB J. 10: 403-412

Dowgert MF, Steponkus PL (1994) "Behaviour of the plasma – membrane of isolated protoplasts during a freeze thaw cycle." Plant Physiol 75(4): 1139-1151

Duin RPW (2000) PRTools- version 3.0- A matlab toolbox for pattern recognition

Duysens LNM, Sweers HE (1963) "Mechanism of two photochemical reactions in algae as studied by means of fluorescence. In: Japanese Society of Plant Physiologists (eds) Studies on microalgae and photosynthetic bacteria." University of Tokyo Press, 353–371

Ehlert B, Hincha DK (2008) "Chlorophyll fluorescence imaging accurately quantifies freezing damage and cold acclimation responses in Arabidopsis leaves." Plant Methods 4(1): 12

El-Faki MS, Zhang N, Peterson DE (2000) "Weed detection using color machine vision." Trans ASAE 43(6):1969-1978

Felton WL, McCloy KR (1992) "Spot spraying." Agric Eng 73(6):9-12

Feyaerts F, van Gool L (2001) "Multi-spectral vision system for weed detection." Pattern Recognit Lett 22(6-7):667-674

Fisher R (1936) "The use of multiple measurements in taxonomic problems." Ann Eugen 7179-188

Flexas J, Bota J, Escalona JM, Sampol B, Medrano H (2002) "Effects of drought on photosynthesis in grapevines under field conditions: an evaluation of stomatal and mesophyll limitations." Funct. Plant Biol. 29: 461–471

Franck F, Juneau P, Popovic R. 2002. Resolution of the Photosyste I and Photosystem II contributions to chlorophyll fluorescence of intact leaves at room temperature. Biochimica et Biophysica Acta 1556, 239–246

Franz E, Gephardt MR, Unklesbay KB (1995) "Algorithms for extracting leaf boundary information from digital images of plant foliage." Trans ASAE 38(2):625-633

Fukunaga K, Hostetler LD (1975) "K-nearest-neighbor bayes-risk estimation." IEEE Trans Inf Theory 21(3):285-293

Fukunaga K (1990) "Introduction to statistical pattern recognition" 2nd ed. Academic Press Professional, San Diego, USA

Genty B, Briantais JM, Baker NR (1989) "The relationship between the quantum yield of photosynthetic electron transport and quenching of chlorophyll fluorescence." Bioch Biophys Acta 990: 87–92

Gerhards R, Kuhbauch W (1993) "Dynamic decision-model for weed control methods in cereals by means of digital image analysis." J Agron Crop Sci 171(5):329-335

Gerhards R, Christensen S (2003) "Real-time weed detection, decision making and patch spraying in maize, sugar beet, winter wheat and winter barley." Weed Res 43(6):385-392

Golub TR, Slonim DK, Tamay, P (1999) "Molecular classification of cancer: Class discovery and class prediction by gene expression monitoring." Science 286(5439): 531–537

Govindjee (1995) 63 years since Kautsky - "Chlorophyll a fluorescence." Aust J Plant Physiol 22(2):131-160

Govindjee, Kern JF, Messinger J, Whitmarsh J (2010) "Photosystem II, in: Encyclopedia of Life Sciences (ELS)." John Wiley & Sons, Ltd.: Chichester,2010. 10.1002/9780470015902.a0000669.pub2.http://www.life.illinois.edu/govindjee/recent_papers.html

Granier C, Aguirrezabal L, Chenu K, Cookson SJ, Dauzat M, Hamard P, Thioux JJ, Rolland G, Bouchier-Combaud S, Lebaudy A, Muller B, Simonneau T, Tardieu F (2006) "PHENOPSIS, an automated platform for reproducible phenotyping of plant responses to soil water deficit in Arabidopsis thaliana permitted the identification of an accession with low sensitivity to soil water deficit." New Phytol 169: 623–635.

Grossweiner LI, Smith KC (1989) "Photosynthesics. In: the scienceof photobiology 2nd ed (Smith KC ed)."Plenum press, New York, 47-78

Hacker J, Spindelbock JP, Neuner G (2008) "Mesophyll freezing and effects of freeze dehydration visualized by simultaneous measurement of IDTA and differential imaging chlorophyll fluorescence." Plant Cell Environ 31(11): 1725–1733

Haggar RJ, Stent CJ, Isaac S (1983) "A prototype hand-held patch sprayer for killing weeds, activated by spectral differences in crop weed canopies." J Agric Eng Res 28(4):349-358

Hannah MA, Wiese D, Freund S, Fiehn O, Heyer AG, Hincha DK (2006) "Natural genetic variation of freezing tolerance in Arabidopsis." Plant Physiol 142(1): 98-112

Haupt-Herting S, Fock HP (2002) "Oxygen exchange in relation to carbon assimilation in water stressed leaves during photosynthesis." Ann Bot 89: 851–859.

Heidarvand L, Amiri RM (2010) "What happens in plant molecular responses to cold stress?" Acta Physiol Plant 2010; 32:419–431

Heijden FVD, Duin RPW, Ridder Dde, Tax DMJ (2004) "Classification, Parameter Eestimation and State Estimation. An Engineering Approach using MATLAB." John Wiley & Sons Ltd, The Atrium, Southern Gate, Chichester, West Sussex PO19 8SQ, England

Heldt HW (1997) "Plant Biochemistry & Molecular Biology." Oxford University Press, Oxford

Hincha DK, Sieg F, Bakaltcheva I, Köth H, Schmitt JM (1996) "Freeze–thaw damage to thylakoid membranes: specific protection by sugars and proteins. In: Steponkus PL, ed. Advances in low-temperature biology." London: JAI Press, 1996;141-183

Hincha DK (2002) "Cryoprotectin: a plant lipid-transfer protein homologue that stabilizes membranes during freezing." Philos T R Soc B 357: 909 – 915

Hjellstrom M, Olsson ASB, Engstrom P, Soderman EM (2003) "Constitutive expression of the water deficit-inducible homeobox gene ATHB7 in transgenic Arabidopsis causes a suppression of stem elongation growth." Plant Cell Environ 26: 1127–1136

Holt NE, Zigmantas D, Valkunas L, Li XP, Niyogi KK, Fleming GR (2005) "Carotenoid cation formation and the regulation of photosynthetic light harvesting." Science, 307: 433–436

Horton P, Ruban AV (1992) "Regulation of photosystem-II." Photosynth Res 34(3):375–385

Hughes TR, Marton MJ, Jones AR (2000) "Functional discovery via a compendium of expression profiles." Cell 102(1): 109–126

Iannacone R, Mittempergher F, Morelli G, Panio G, Perito A, Ruberti I, Sessa G, Cellini F (2008) "Influence of an Arabidopsis dominant negative ATHB2 mutant on tomato plant development." Acta Hort 789: 263-276

Iftime D, Hannah MA, Peterbauer T, Heyer AG (2011) "Stachyose in the cytosol does not influence freezing tolerance of transgenic Arabidopsis expressing stachyose synthase from adzuki bean." Plant Sci 180(1): 24–30

Jain AK, Mao JC, Mohiuddin KM (1996) "Artificial neural networks: A tutorial." Computer 29(3):31-44

Jain AK, Duin RPW, Mao JC (2000) "Statistical pattern recognition: A review." IEEE Trans Pattern Anal Mach Intell 22(1):4-37

Jansen M, Gilmer F, Biskup B, Nagel KA, Rascher U, Fischbach A, Briem S, Dreissen G, Tittmann S, Braun S, De Jaeger I, Metzlaff M, Schurr U, Walter A (2009) "Simultaneous phenotyping of leaf growth and chlorophyll fluorescence via GROWSCREEN FLUORO allows detection of stress tolerance in Arabidopsis thaliana and other rosette plants." Funct Plant Biol 36: 902–914

Jayas DS, Paliwal J, Visen NS (2000) "Multi-layer neural networks for image analysis of agricultural products." J Agric Eng Res 77(2):119-128

Joliet P, Johnson GN (2011)"Regulation o cyclic and linear electron flow in higher plants."www.pnas.org/lookup/suppl/doi:10.1073/pnas.1110189108/-/DCSupplemental

Jongdee B, Fukai S, Cooper M (2002) "Leaf water potential and osmotic adjustment as physiological traits to improve drought tolerance in rice." Field Crops Res 76: 153-163

Kautsky H, Hirsch A (1931) "Neue Versuche zur Kohlensäureassimilation". Naturwissenschaften 19:964

Kavdir I (2004) "Discrimination of sunflower, weed and soil by artificial neural networks." Comput Electron Agric 44(2):153-160

Kawakami K, Umena Y, Kamiya N, Shen JR (2011) "Structure of the catalytic, inorganic core of oxygen-evolving photosystem II at 1.9 angstrom resolution." J photoco photobio B, 104 (1-2): 9-18

Keranen M, Aro EM, Tyystjarvi E, Nevalainen O (2003) "Automatic plant identification with chlorophyll fluorescence fingerprinting." Precis Agric 4(1):53-67

Kirkham MB (1977) "Water potential and turgor pressure as a selection basis for wind-grown winter wheat." Agr Water Manage 1: 343-349

Kitajima K, Hogan KP (2003) "Increases of chlorophyll a/b ratios during acclimation of tropical woody seedlings to nitrogen limitation and high light."Plant cell and environment, 26: 857-865

Kitajima M, Butler WL (1975) "Quenching of chlorophyll fluorescence and primary photochemistry in chloroplasts by dibromothymoquinone." Biochim. Biophys. Acta 376: 105-115

Kittler J (1978) "Feature set search algorithms." Pattern Recognit Signal Process 41-60

Koornneef M, Jorna ML, Derswan DLCB, Karssen CM (1982) "The isolation of abscisic acid (ABA) deficient mutants by selection of induced revertants in non germinating gibberellin sensitive lines of Arabidopsis thaliana (L.) Heynh." Theor Appl Genet 61: 385– 393

Krause GH, Somersalo S (1989) "Fluorescence as a tool in photosynthesis research: Application in studies of photoinhibition, cold acclimation and freezing stress." Philos T R Soc B 323 (1216): 281-293

Krause GH, Weis E (1991)" Chlorophyll fluorescence and photosynthesis: the basics." Ann Rev Plant Physiol Plant Mol Biol 42:313– 349

Krause G, Jahns P (2004) "Non-photochemical energy dissipationdetermined by chlorophyll fluorescence qenching: characterization and function. In: Papgeorgiou G, Govindjee (eds,) chlorophyll a fluorescence: A signature of photosynthesis." Springer, Dordrecht

Külheim C,Agren J, Jansson S (2002) "Rapid regulation of light harvesting and plant fitness in the field." Science, 297: 91-93

Lau KW, Wu QH (2003) "Online training of support vector classifier." Pattern Recognit 36(8):1913-1920

Lazàr D (1999) "Chlorophyll a fluorescence induction." Biochim Biophys Acta 1412:1–28

Lazàr D, Susila P, Naus J (2006) "Early detection of plant stress from changes in distributions of chlorophyll a fluorescence parameters measured with fluorescence imaging." J Fluoresc 16(2):173-176

Lee WS, Slaughter DC, Giles DK (1999) "Robotic weed control system for tomatoes." Precis Agric 195-113

Leegood R, Sharkey T, von Caemmerer S (2000) "Photosynthesis: Physiology and metabolism. Series: Govindjee (ed.) Advances in photosynthesis." Kluwer Academc Publishers, Dordrecht

Leung J, Giraudat J (1998) "Abscisic acid signal transduction." Ann Rev Plant Physiol Plant Mol Biol 49: 199–222

Levitt J (1980) "Responses of plants to the environmental stresses, Water, radiation, salt and other stresses." Vol 2, 2nd Edition Academic Press, New York, 606

Lichtenthaler HK (1987) "Chlorophylls and carotenoids: Pigments of photosynthetic biomembranes." Methods Enzymol. 148:350-382

Lichtenthaler HK, Buschmann C, Knapp M (2005) "How to correctly determine the different chlorophyll fluorescence parameters and the chlorophyll fluorescence decrease ratio R_{Fd} of leaves with the PAM fluorometer." Photosynthetica 43(3):379-393

Mahalanobis PC (1930) "On the tests and measures of group divergences. J Proc Asiatic Soc Bengal 26: 541–588

Malenovský Z, Mishra KB, Zemek F, Rascher U, Nedbal L (2009) "Scientific and technical challenges in remote sensing of plant canopy reflectance and fluorescence." J Exp Bot 60: 2987-3004

Mane SP, Vasquez-Robinet C, Sioson AA, Heath LS, Grene R (2007) "Early PLD alpha - mediated events in response to progressive drought stress in Arabidopsis: a transcriptome analysis." J Exp Bot 58: 241–252

Marler TE, Mickelbart MV (1998) "Drought, leaf gas exchange, and chlorophyll fluorescence of field-grown papaya." J Am Soc Horticul Sci 123: 714–718

Martinez AM, Kak AC (2001) "PCA versus LDA." IEEE Trans Pattern Anal Mach Intell 23(2):228-233

Matouš K, Benediktyova Z, Berger S, Roitsch T, Nedbal L (2006) "Case study of combinatorial imaging: What protocol and what chlorophyll fluorescence image to use when visualizing infection of Arabidopsis thaliana by Pseudomonas syringae?" Photosynth Res 90(3):243-253

Matsubara S, Chen Y-C, Caliandro R, Govindjee , Clegg RM (2011) " Photosystem II fluorescence lifetime imaging in avocado leaves: Contributions of the lutein-epoxide and violaxanthin cycles to fluorescence quenching." J Photochem Photobiol B: Biology 104(1-2) 271–284

Maxwell K, Johnson GN (2000) "Chlorophyll fluorescence: A practical guide." J Exp Bot 51(345): 659–668

McQueen J (1967) "Some methods for classification and analysis of multivariate observations, in proc. of the 5th berkeley symposium on mathematical statistics and probability."

Mishra A, Matouš K, Mishra KB, Nedbal L (2009) "Towards discrimination of plant species by machine vision: advanced statistical analysis of chlorophyll fluorescence transients." J Fluoresc 19(5): 905-913

Mishra A, Mishra KB, Höermiller II, Heyer AG, Nedbal L (2011) "Chlorophyll fluorescence emission as a reporter on cold tolerance in Arabidopsis thaliana accessions." Plant Signal Behav 6(2): 301-310

Mishra KB, Gopal R (2008) "Detection of nickel-induced stress using laser-induced fluorescence signatures from leaves of wheat seedlings." Intern J Remote Sens, 29(1-2): 157-173

Mishra KB, Iannacone R, Petrozza A, Mishra A, Armentano N, Vecchia GL, Trtílek M, Cellini F, Nedbal L (2011) "Engineered drought tolerance in tomato plants is reflected in chlorophyll fluorescence emission." Plant Science, 2011. doi:10.1016/j.plantsci.2011.03.022

Mitchell - Olds T, Schmitt J (2006) "Genetic mechanisms and evolutionary significance of natural variation in Arabidopsis." Nature 441: 947-952

Moffatt B, Ewart V, Eastman A (2006) "Cold comfort: plant antifreeze proteins." Physiol Plant 126: 5–16

Moon BY, Higashi SI, Gombos Z, Murata N (1995) "Unsaturation of the membrane-lipids of chloroplasts stabilizes the photosynthetic machinery against low-temperature photoinhibition in transgenic tomato plants." Proc Natl Acad Sci USA 92: 6219-6223

Munne-Bosch S, Nogues S, Alegre L (1999) "Diurnal variations of photosynthesis and dew absorption by leaves in two evergreen shrubs growing in mediterranean field conditions." New Phytol 144(1):109-119

Munns R, James RA, Sirault XRR, Furbank RT, Jones HG (2010) "New phenotyping methods for screening wheat and barley for beneficial responses to water deficit." J Exp Bot 61: 3499-3507.

Murchie EH, Niyogi KK (2011) "Manipulation of photoprotection to improve plant photosynthesis." Plant physiol, 155: 86-92

Murray MB, Cape JN, Fowler D (1989) "Quantification of frost damage in plant-tissues by rates of electrolyte leakage." New Phytol 113(3): 307-311

Müller P, Li XP and Niyogi KK (2001) "Non-photochemical quenching.A response to excess light energy." Physiol Plant 125: 1558-1566

Nedbal L, Soukupova J, Kaftan D, Whitmarsh J, Trtilek M (2000a) "Kinetic imaging of chlorophyll fluorescence using modulated light." Photosynth Res 66(1-2):3-12

Nedbal L, Soukupová J, Whitmarsh J et. al. (2000b) "Postharvest imaging of chlorophyll fluorescence from lemons can be used to predict fruit quality." Photosynthetica 38, (4):571-579

Nedbal L, Whitmarsh J (2004) "Chlorophyll fluorescence imaging of leaves and fruits. In: Papageorgiu G, Govindjee, eds. Chlorophyll a fluorescence: a signature of photosynthesis." The Netherland: Springer, Dordrecht, 389-407

Nedbal, L. Koblížek M (2006) Chlorophyll fluorescence as a reporter on in vivo electron transport and regulation in plants. In: Grimm B, Porra R,Scheer H (ed) Chlorophylls and Bacteriochlorophylls: Biochemistry, Biophysics, Functions and Applications, Springer, The Netherlands

Neuner G, Buchner O (1999) "Assessment of foliar frost damage: a comparison of in vivo chlorophyll fluorescence with other viability tests." J Appl Bot 73(1-2): 50–54

Neuner G, Pramsohler M (2006) "Freezing and high temperature thresholds of photosystem II compared to ice nucleation, frost and heat damage in evergreen subalpine plants." Physiol Plant 2006; 126 (2): 196–204

Novillo F, Alonso JM, Ecker JR, Salinas J (2004) "CBF2/DREB1C is a negative regulator of CBF1/DREB1B and BF3/DREB1A expression and plays a central role in stress tolerance in Arabidopsis." Proc Natl Acad Sci USA 101 (11): 3985–3990

Ohashi Y, Nakayama N, Saneoa H, Fujita H (2006) "Effects of drought stress on photosynthetic gas exchange, chlorophyll fluorescence and stem diameter of soybean plants." Biol Plant 50:138-141

Oliver DJ (1998) :Photorespiration and the C2 cycle. In: Photosynthesis: A Comprehensive Treatise (ed.A. S.Raghavendra)." Cambridge University Press,Cambridge, 173–182

Omasa K, Shimazaki KI, Aiga I, Larcher W and Onoe M (1987) "Image analysis of chlorophyll fluorescence transcients for diagnosing the photosynthetic system of attached leaves." Plant physiol 84, 748-752

Omasa K, Takayama K (2003) "Simultaneous measurement of stomatal conductance, non-photochemical quenching, and photochemical yield of photosystem II in intact leaves by thermal and chlorophyll fluorescence imaging." Plant Cell Physiol 44: 1290-1300

Ort DR, Baker NR (2002)"A photoprotective role for O-2 as an alternative electron sink in photosynthesis?" Curr Opin Plant Biol 5: 193-198

Oxborough K (2004) "Imaging of chlorophyll fluorescence: theoretical and practical aspects of an emerging technique for the monitoring of photosynthetic performance." J Exp Bot 55 (400) 1195-1205

Ögren E, Öquist G (1885) "Effects of drought on photosynthesis, chlorophyll fluorescence and photoinhibition susceptibility in intact willow leaves." Planta 166: 380–388

Ögren E (1990) "Evaluation of chlorophyll fluorescence as a probe for drought stress in willow leaves." Plant Physiol 93: 1280–1285

Öquist G, Huner NPA (1993) "Cold hardening induced resistance to photoinhibition in winter rye is dependent upon an increase capacity for photosynthesis." Planta 189: 150-156

Paclik P, Duin RPW (2003) "Dissimilarity-based classification of spectra: computational issues." Real Time Imaging 9(4): 237-244

Papageorgiou GC, Govindjee (2004) "Chlorophyll a fluorescence: A signature of photosynthesis" Advances in photosynthesis and respiration, Springer, Dordrecht, The Netherlands

Papageorgiou GC, Tsimilli-Michael M, Stamatakis K (2007) "The fast and slow kinetics of chlorophyll a fluorescence induction in plants, algae and cyanobacteria: a viewpoint." Photosynth Res 94: 275–290

Park S, Li JS, Pittman JK, Berkowitz GA, Yang HB, Undurraga S, Morris J, Hirschi KD, Gaxiola RA (2005) "Up-regulation of a H+-pyrophosphatase (H+-PPase) as a strategy to engineer drought-resistant crop plants." Proc Natl Acad Sci USA 102: 18830-18835

Peguero-Pina JJ, Morales F, Gil-Pelegrin E (2008) "Frost damage in Pinus sylvestris L. stems assessed by chlorophyll fluorescence in cortical bark chlorenchyma." Ann For Sci 65(8):1-6

Pekalska E, Duin RPW (2001) "On Combining Dissimilarity Representations ", on "Multiple Classifier System" Second International Workshop. " MCS 2001 Cambridge, UK, 359-368

Pfündel E (1998) "Estimating the contribution of photosystem I to total leaf chlorophyll fluorescence." Photosynth Res 56: 185–195

Pospisilova J (1988) "Osmotic adjustment in tobacco plantlets." Biol Plantarum, 30: 393-396

Pospíšil P, Skotnica J, Nauš J (1998) "Low and high temperature dependence of minimum F_0 and maximum F_m chlorophyll fluorescence in vivo." Biochimica et Biophysica Acta 1363(2): 95–99

Pudil P, Novovicova J, Kittler J (1994) Floating search methods in feature selection." Pattern Recognit Lett 15(11):1119-1125

Rajendran K, Tester M, Roy SJ (2009) "Quantifying the three main components of salinity tolerance in cereals." Plant Cell Environ 32: 237–249

Rapacz M (2007) "Chlorophyll a fluorescence transient during freezing and recovery in winter wheat." Photosynthetica 45(3): 409-418

Rapacz M, Woźniczka A (2009) "A selection tool for freezing tolerance in common wheat using the fast chlorophyll a fluorescence transcients." Plant Breeding 128(3):227-234

Rascher U, Nedbal, L (2006) "Dynamics of plant photosynthesis in fluctuating light." In: Curr Opin Plant Biol (9): 671-678

Ren TI (2000) "Rattern recognition, In: Pattern Recognition and Complex System" University Antwerpen, PhD thesis, 9-16

Reyes-Díaz M, Ulloa N, Zúniga-Feest A, Gutiérrez A, Gidekel M, Alberdi M, Corcuera LJ, Bravo LA (2006) "Arabidopsis thaliana avoids freezing by supercooling." J Exp Bot 57 (14): 3687–3696

Riga P, Vartanian N (1999) "Sequential expression of adaptive mechanisms is responsible for drought resistance in tobacco." Austr J Plant Physiol 26: 211-220

Rizza F, Pagani D, Stanca AM, Cattivelli L (2001) "Use of chlorophyll fluorescence to evaluate the cold acclimation and freezing tolerance of winter and spring oats." Plant Breeding 120 (5):389-396

Roháček K (2002) "Chlorophyll fluorescence parameters: the definitions, photosynthetic meaning, and mutual relationships." Photosynthetica 40: 13-29

Rohde P, Hincha DK, Heyer AG (2004) "Heterosis in the freezing tolerance of crosses between two Arabidopsis thaliana accessions (Columbia-0 and C24) that show differences in non-acclimated and acclimated freezing tolerance." Plant J 38(5):790-799

Rumich-Bayer S, Krause GH (1986) "Freezing damage and frost tolerance of the photosynthetic apparatus studied with isolated mesophyll protoplasts of Valerianella locusta L." Photosynth Res 8(2): 161-174

Rundel RD. 1983. Action spectra and estimation of biologically effective UV radiation. Physiologia Plantarum 58, 360–366

Schreiber U, Schliwa U, Bilger W (1986) "Continuous recording of photochemical and nonphotochemical chlorophyll fluorescence quenching with a new type of modulation fluorometer." Photosyn Res 10: 51-62

Schreiber U (2004) "Pulse-Amplitude-Modulation (PAM) Fluorometry and Saturation Pulse Method: An Overview(Chapter 11) "Chlorophyll a Fluorescence a Signature of Photosynthesis", edited by GeorgePapaqeorgiou and Govindjee." Springer,Dordrecht, TheNetherlands, 279-319

Scotford IM, Miller PCH (2005) "Applications of spectral reflectance techniques in northern european cereal production: A review." Biosyst Eng 90(3):235-250

Sharma KK, Lavanya M (2002) "Recent developments in transgenics for abiotic stress in legumes of the semi-arid tropics." In: M. Ivanaga (Ed.), Genetic Engineering of Crop Plants for Abiotic Stress. Working Report No. 23, JIRCAS, Tsukuba , Japan, 61-73

Shiraishi M, Sumiya H (1996) "Plant identification from leaves using quasi-sensor fusion." J Manuf Sci Eng Trans ASME 118(3):382-387

Siedlecki W, Sklansky J (1989) "A note on genetic algorithms for large-scale feature selection." Pattern Recognit Lett 10(5):335-347

Smallwood M, Bowles DJ(2002) "Plants in a cold climate." Philos T R Soc B 357: 831-846

Söderman E, Mattsson J, Svenson M, Borkird C, Engström P (1994) "Expression patterns of novel genes encoding homeodomain leucine-zipper proteins in Arabidopsis thaliana." Plant Mol Biol 26: 145–154

Söderman E, Mattsson J, Engström P (1996) "The Arabidopsis homeobox gene ATHB-7 is induced by water deficit and by abscisic acid." Plant J 10: 375–381

Somerville C, Briscoe L (2001) "Genetic Engineering and Water." Science 292 (2001) 2217.

Somol P, Pudil P, Kittler J (2004) "Fast branch & bound algorithms for optimal feature selection." IEEE Trans Pattern Anal Mach Intell 26(7):900-912

Stapleton AE, Walbot V (1994) "Flavonoids can protect maize DNA from the induction of ultraviolet radiation damage." Plant Physiol, 105: 881-889

Steponkus PL (1984)"Role of the plasma membrane in freezing-injury and cold acclimation." Annu Rev Plant Physiol Plant Mol Biol 35: 543-584

Steponkus PL, Lynch DV, Uemura M (1990) "The influence of cold-acclimation on the lipid-composition and cryobehavior of the plasma-membrane of isolated rye protoplasts." Philos T R Soc B 326(1237): 571-583

Stirbet A, Govindjee (2011) "On the relation between the Kautsky effect (chlorophyll a fluorescence induction) and Photosystem II: Basics and applications of the OJIP fluorescence transient." J Photochem Photobiol B: Biol (in press), doi:10.1016/j.jphotobiol.2010.12.010

Stitt M, Hurry V. A (2002) "plant for all seasons: alteration in photosynthetic carbon metabolism during cold acclimation in Arabidopsis." Curr Opin Plant Biol 5:199-206

Strand A, Hurry V, Henkes S, Huner N, Gustafsson P, Gardeström P, Stitt M (1999) "Acclimation of Arabidopsis leaves developing at low temperature: Increasing cytoplasmic volume accompanies increased activities of enzymes in the Calvin cycle and in the sucrose-biosynthesis pathway." Plant Physiol 119:1387-1397

Strasser A, Arnaud H, Baudin F, Röhl U (1995) "Small-scale shallow-water carbonate sequences of Resolution Guyot (Sites 866, 867, and 868)." Proc ODP, Sci, 143: 119-131

Strasser A, Hillgärtner H (1998) "High-frequency sea-level fluctuations recorded on a shallow carbonate platform (Berriasian and Lower Valanginian of Mount Salève, French Jura)." Eclogae geol Hely, 91: 375-390

Strasser RJ, Srivastava A, Tsimilli-Michael M (2004) "Analysis of the chlorophyll a fluorescence transient. In: G. Papageorgiou and Govindjee, Editors, Chlorophyll Fluorescence: A Signature of Photosynthesis, Advances in Photosynthesis and Respiration." Kluwer Academic Publishers, The Netherlands 9: 321–362

Takeda S, Matsuoka M (2008) "Genetic approaches to crop improvement: responding to environmental and population changes." Nat Rev Genet 9:444-457

Theodoridis S, Koutroumbas K (2009) "Pattern recognition (4th ed.)." Elsevier Inc., USA

Thomas JB, Voskuil W, Olsman H, De Boois HM (1962) "Fluorescence- induction phenomena in isolated chloroplasts." Biochim Biophys Acta 59:224–226.

Thomson JA (2002) "Research needs to improve agricultural productivity and food quality, with emphasis on biotechnology." J Nutr 132: 3441S–3442S.

Tian LF, Slaughter DC (1998) "Environmentally adaptive segmentation algorithm for outdoor image segmentation." Comput Electron Agric 21(3):153-168

Timmermann C, Gerhards R, Kuhbauch W (2003) "The economic impact of site-specific weed control." Precis Agric 4(3):249-260

Tong AH, Lasage G, Bader GD (2004) "Global mapping of the yeast genetic interaction network." Science 303(5659): 808–813

Trewavas AJ, Jones HG (1991) "An assessment of the role of ABA in plant development" In: Davies WJ,, Jones HG (Eds.), Abscisic Acid: Physiology and Biochemistry, BIOS. Scientific Publishers, Oxford, UK, 169-188

Turner NC, Wright GC, Siddique KHM (2001) "Adaptation of grain legumes (pulses) to water limited environments." Adv Agron 71: 193 – 231

Tyystjärvi E, Koski A, Keranen M, Nevalainen O (1999) "The Kautsky curve is a built-in barcode." Biophys J 77(2):1159-1167

Umena Y, Kawakami K, Shen JR, Kamiya N (2011) "Crystal structure of oxygen-evolving photosystem II at a resolution of 1.9 angstrom ." nature, 473(7345): 55-65

Umezawa T, Fujita M, Fujita Y, Yamaguchi-Shinozaki K, Shinozaki K (2006) "Engineering drought tolerance in plants: discovering and tailoring genes to unlock the future." Curr Opin Plant Biotech 17: 113-122

Valliyodan B, Nguyen HT (2006) "Understanding regulatory networks and engineering for enhanced drought tolerance in plants." Curr Opin Plant Biol 9: 189-195

Vrindts E, De Baerdemaeker J (2000) "Using spectral information for weed detection in field circumstances." AgEng 2000 Conference. Warwick, UK

Wang N, Zhang N, Dowell FE, Sun Y, Peterson DE (2001) "Design of an optical weed sensor using plant spectral characteristics." Trans ASAE 44(2):409-419

Wang XC, Paliwal KK (2003) "Feature extraction and dimensionality reduction algorithms and their applications in vowel recognition." Pattern Recognit 36(10):2429-2439

Whitfield CW, Cziko AM, Robinson GE (2003)"Gene expression profiles in the brain predict behavior in individual honey bees." Science 302(5643): 296–299

Whitehead D, Walcroft AS, Scott NA, Townsend JA, Trotter CM, Rogers GND (2004) "Characteristics of photosynthesis and stomatal conductance in the shrub land species manuka (Leptospermum scoparium) and kanuka (Kunzea ericoides) for the estimation of annual canopy carbon uptake." Tree Physiol 24(7):795–804

Wildman SG, Jope CA, Atchison BA (1980) "Light microscopic analysis of the three-dimensional structure of higher plant chloroplasts. position of starch grains and probable spiral arrangement of stroma lamellae and grana." Botanical Gazette, 141: 24-36

Woo NS, Badger MR, Pogson BJ (2008) "A rapid, non-invasive procedure for quantitative assessment of drought survival using chlorophyll fluorescence." Plant Methods 27: 4

Yamamoto HY, Bassi R (1996) Carotenoids: localization and function. In Oxygenic Photosynthesis: The Light Reactions (Ort DR, Yocum CF, eds.) Advances in Photosynthesis 4, Kluwer, Dordrecht

Yang SJ, Vanderbeld B, Wan JX, Huang YF (2010) "Narrowing down the targets: Towards successful genetic engineering of drought-tolerant crops." Mol Plant *3: 469-490*

Yoon HS, Soh J, Min B, Yang HS (1999) "Recognition of Alphabetical Hand Gestures Using Hidden Markov Model." IEICE Transactions Fundamentals E82-A(7): 1358-1366

Young AJ (1993) Occurrence and distribution of carotenoids in photosynthetic systems. In Carosenoids in Photosynthesis (Young A, Britton mis. G)." Chapman and Hall, London, 16-71

Zhang JZ, Creelman RA, Zhu JK (2004) "From laboratory to field. Using information from Arabidopsis to engineer salt, cold, and drought tolerance in crops." Plant Physiol 135: 615–621

Zhen Y, Ungerer MC (2008) "Relaxed selection on the CBF/DREB1 regulatory genes and reduced freezing tolerance in the southern range of Arabidopsis thaliana." Mol Biol Evol 25 (12):2547-2555

Websites:

http://www.life.illinois.edu/govindjee/paper/fig5.gif
http://classroom.sdmesa.net/eschmid/Lecture19-Microbio.htm
http://pcp.oxfordjournals.org/content/45/1/92/F1.expansion
http://www.answersingenesis.org/articles/tj/v17/n3/photosynthesis
http://www.uic.edu/classes/bios/bios100/f06pm/lect08.htm
http://en.wikipedia.org/wiki/File:Thylakoid_membrane.png
http://en.wikipedia.org/wiki/Calvin_cycle
http://www.olympusmicro.com/primer/java/jablonski/jabintro/index.html
http://en.wikipedia.org/wiki/Euclidean_distance
http://www.aiaccess.net/English/Glossaries/GlosMod/e_gm_mahalanobis.htm
http://cmp.felk.cvut.cz/cmp/courses/recognition/Labs/perceptron/index_en.html
http://www.springerimages.com/Images/LifeSciences/5-10.1186_1471-2105-7-73-3
http://zone.ni.com/reference/enXX/help/372916H01/nivisionconcepts/classification_methods/
http://www.emeraldinsight.com/journals.htm?articleid=870666&show=html
www.psi.cz
http://www.graphpad.com
http://www.prtools.org/
http://www.life.illinois.edu/govindjee/recent_papers.html

7. Appendixes

Images for the nine accessions of *Arabidopsis thaliana*

Accessions in group of three


Ler
Nd
Can


C24
Co
Cvi